J. Webster (ed.), *Wiley Encyclopedia of Electrical and Electronics Engineering*
Copyright © 1999 John Wiley & Sons, Inc.

SUPERCONDUCTORS, FORCED FLOW CONDUCTOR MANUFACTURING

Electric windings that use low temperature superconductors need to be actively cooled. An easy and effective way to maintain the winding at operating temperature is to fill the space around the coil with liquid helium (pool-cooled magnets), allowing the liquid to penetrate between the turns. Alternatively, the superconductor may include a cooling path where the coolant is forced to circulate under pressure. This article is a review of the manufacturing methods for forced flow conductors, starting from the early prototypes (30 years ago) to the very large cable-in-conduit conductors of the fusion magnets. The design aspects of forced flow conductors are not deeply discussed here, although they have sometimes driven the effort toward advanced manufacturing technologies. Essential references on the design aspects of forced flow conductors can be found in the articles Superconductors, STABILITY IN FORCED FLOW CONDUCTORS; HYSTERESIS AND COUPLING LOSSES IN SUPERCONDUCTORS; AND SUPERCONDUCTING MAGNETS, QUENCH PROTECTION.

The manufacturing methods for forced flow superconductors sound like a brand new subject. Actually, it is old enough to have a history. The initial proposal dates back to 1965, when 1 suggested using the circulation of supercritical helium for reliable cooldown and heat transfer in large superconducting magnets. The first milestone is the spark chamber detector built in 1970 at CERN (2), with 50 MJ stored energy and 24 tonnes of NbTi hollow conductor.

Besides the clear advantage in thermal behavior, a key argument in favor of forced flow conductors is electromechanical integrity. In contrast with pool-cooled windings, where the individual turns are insulated only by spacers to allow the coolant to wet the metallic surface, the turns of a winding made of forced flow conductor can be fully insulated and potted. Such a rigid structure offers superior mechanical performance under electromagnetic load and withstands very high operating voltages (e.g., in pulsed or quench mode), not limited by the dielectric strength of the coolant. Clearly, the choice of forced flow conductors becomes mandatory for magnets with very large stored energy, subjected to high operating loads and requiring high-voltage discharge in case of quench.

Comparing the latest forced flow conductors with the early ones, manufactured thirty years ago, the difference is impressive. On one side, the conductor design has made substantial progress, using the results of extensive R&D work (mostly on ac loss and stability) and sophisticated thermohydraulic codes. On the other, the manufacturing methods have evolved under the pressure of the design goals, and advanced technologies have become reliable and affordable.

The present review is focused on the manufacturing aspects. In general, only practical industrial manufacturing experience is quoted; short prototype conductors are reported only if an original method was used. The review is organized in three main sections. The first describes the conductor generation where the helium flows in smooth pipes and the superconductor is attached outside the pipes, without direct contact with the coolant. The second generation is a transition group of conductors, where a flat cable is encased in a welded steel sheath. The third generation includes the rope-in-pipe, or cable-in-conduit, conductors, where the coolant is forced to flow through a bundle of strands with large void fraction, encased in a structural conduit.

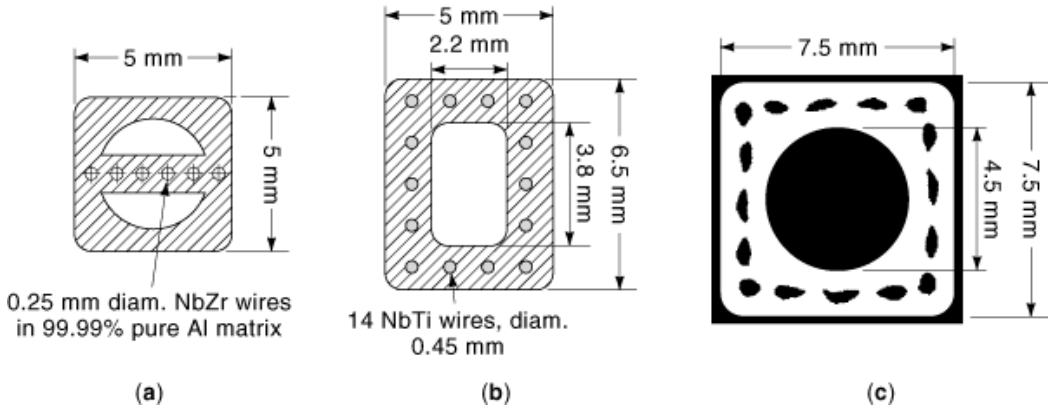

Fig. 1. Three extruded hollow superconductors: (a) Al matrix with NbZr filaments (1967, courtesy of CERN), (b) Cu matrix with NbTi filaments (IMI, 1968), (c) round in square Cu matrix with thick NbTi filaments (MFO, later ABB, about 1968).

Superconducting cables for power transmission lines are not in the scope of this review. Their manufacturing methods, dominated by the high-voltage insulation requirements, are similar to those for conventional high-voltage conductors for underground lines.

Conductors with Smooth Pipes

In the late sixties, the use of a helium-tight conduit produced by extended welded seams was considered too risky for large-scale applications (particle detectors, fusion magnets), where a single leak in the winding would have either severely delayed or compromised the entire project. It is understandable that copper pipes were initially selected for forced flow conductors, because of their high thermal conductivity, small pressure drop, and reliable leak-tightness.

Four conductor subgroups are identified according to the assembly procedure for attaching the superconductor to the copper pipes.

Superconducting Pipes. The first experiments with forced flow conductors look today like small masterpieces of technology. The idea was not to attach a superconducting wire to a pipe, but to create a hole in a superconducting composite.

A cross section of the first ever reported hollow superconductor is shown in Fig. 1(a). The extruded composite has a pure aluminum matrix with six NbZr filaments (0.25 mm thick) in the midplane, to allow bending radii down to 10 mm. The copper-plated NbZr filaments were supplied by Supercon (United States), and the hollow extrusion was done in 1967 at the Atelier électroméchanique de Gascogne (France). Over 300 m of conductor have been produced and successfully wound into a solenoid at CERN (3).

The hollow conductor shown in Fig. 1(b) was commercially produced by Imperial Metal Industries (England) at the end of the sixties. The rectangular, extruded pipe, 6.5 $\times$ 5 mm, is made of copper, with 14 NbTi filaments (0.45 mm diam) embedded in it. The production lengths ranged up to 200 m. At CERN, the conductor sections were electron beam welded (4) and wound into a solenoid of 32 double pancakes, for a total of 2500 m of conductor. At Saclay, France, a smaller, racetrack coil (5) was wound with 300 m of the same conductor.

At M.F.O. (Switzerland), later BBC and ABB, a larger, square superconducting pipe was developed (6) by hollow extrusion of a copper billet with 16 NbTi filament ($\approx$ 0.55 mm diameter); see Fig. 1(c). Because of the large cross section, the conductor unit length was limited to 100 m.

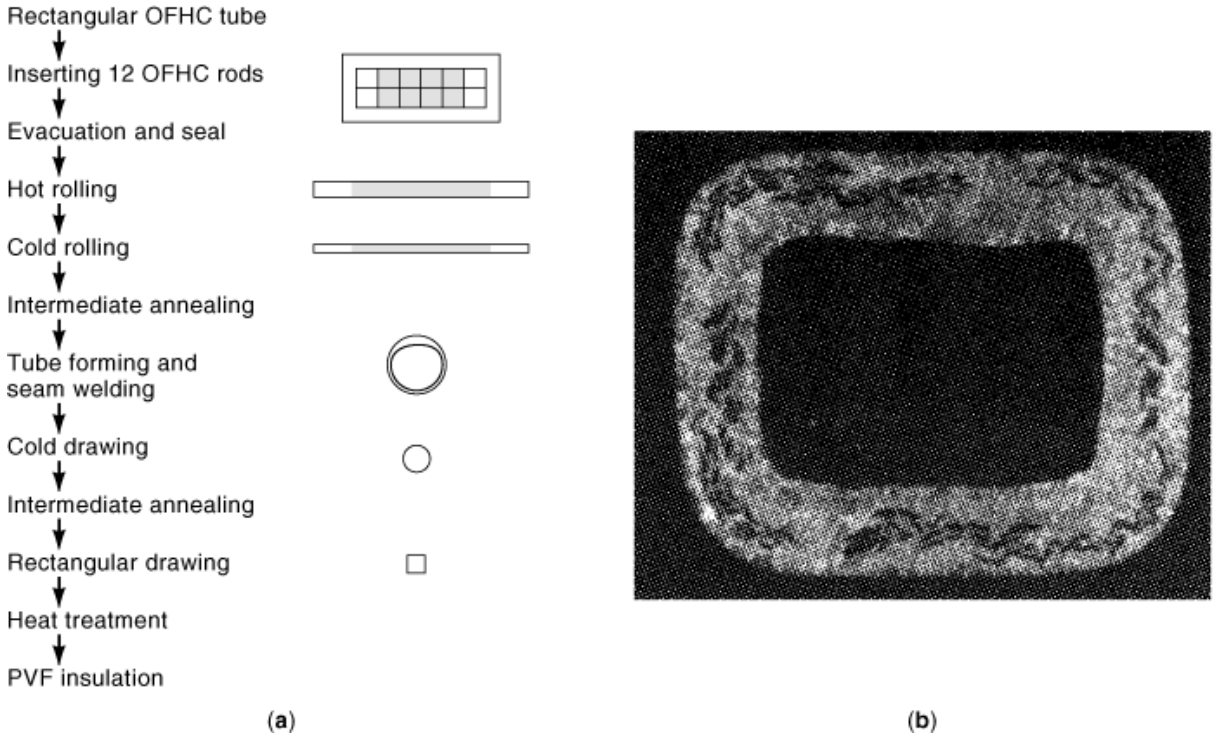

Fig. 2. A hollow superconductor (7), manufacture in 1974 by a tube mill method (courtesy of K. Agatsuma, *ETL*, Japan).

The manufacture of a hollow superconductor at the Electro-Technical Laboratory, Tsukuba, Japan (*ETL*) was reported in 1974 (7). The method is shown schematically in Fig. 2(a). Twelve square rods of superconducting composite (6 × 6 mm), each with 19 NbTi filaments in a copper matrix, were inserted in a rectangular copper tube and rolled with intermediate annealing to a flat strip, 1.6 mm thick. The strip was then welded in a conventional tube mill and drawn down to form a rectangular hollow conductor, 4 × 5 mm; see Fig. 2(b). Due to the rolling process, the 116 filaments, with equivalent diameter 0.25 mm, are flattened and nonhomogeneously spaced.

The major drawbacks of such "superconducting pipes" are the large size (leading to poor critical current density) of the superconducting filaments due to the limited reduction ratio, and their nontransposition with respect to the transverse field, due to the lack of twisting. As a result, large flux jumps were observed in operation.

Conductors Assembled by Electroplating. An original method was developed at the Kurchatov Institute (Moscow) in the late sixties to bond together the superconducting strands into large composites by continuous electroplating in a $CuSO_4$ electrolyte (8). The same method was later used to assemble the force flow conductors for the toroidal coils of the Tokamak-7 (T-7) and Tokamak-15 (T-15).

The T-7 conductor (9) is made from a linear array of nine copper pipes, 2 mm inner diameter, with 16 multifilamentary NbTi strands sitting in the grooves between the pipes; see Fig. 3(a). Another 32 thin, single core NbTi wires are placed in the grooves between the multifilamentary strands and the copper pipes to obtain an even surface. The pipe–strands assembly is bonded by electroplating a 0.6 mm copper layer up to the final size of 28 × 4.5 mm. The strands are not transposed, and the conductor has suffered from severe flux jumps, triggering quenches during ramp up and down. The large number of parallel cooling channels, supplied by two-

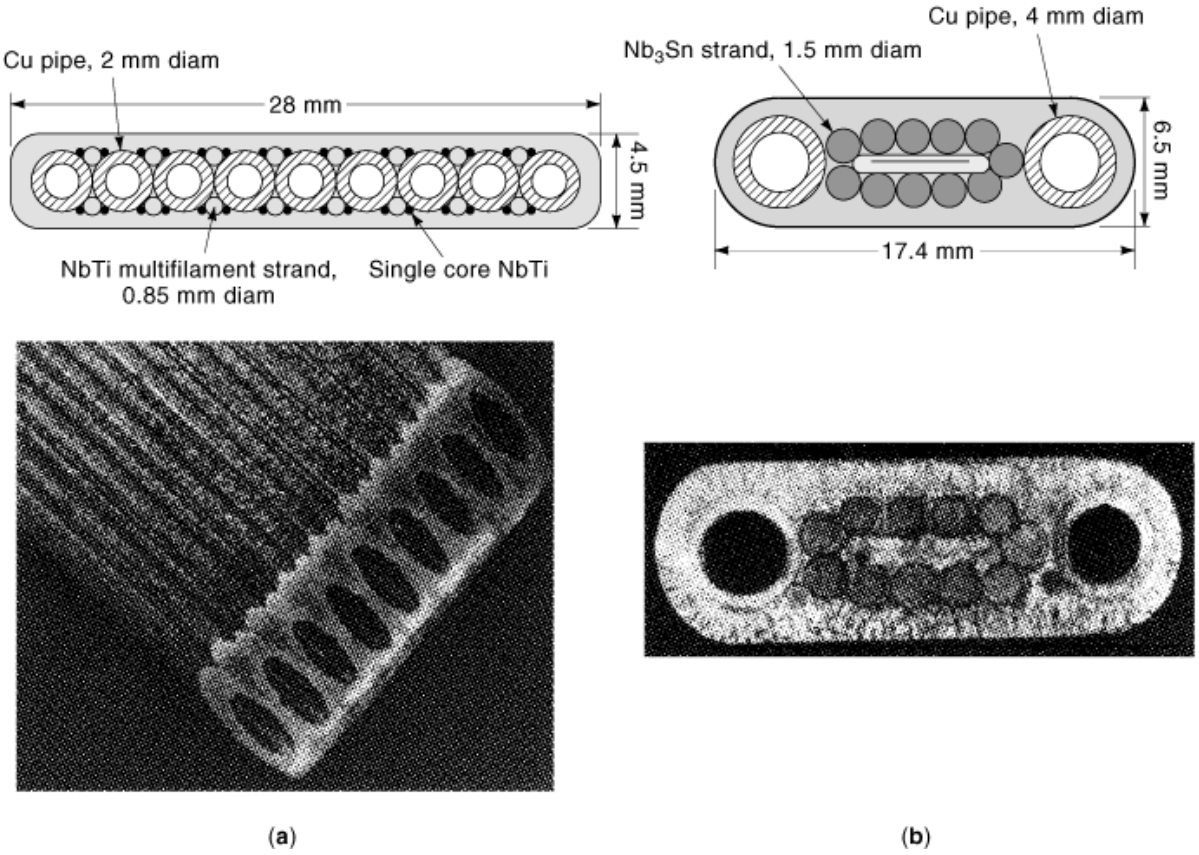

Fig. 3. Cross section of the conductors assembled by copper electroplating at Kurchatov Institute: (a) the NbTi-based T-7; (b) the react-and-wind Nb_3 Sn conductor for the T-15. (Courtesy of Kurchatov and Bochvar Institutes, Moscow.)

phase helium, results in a highly nonhomogenous distribution of the mass flow rate. Over 10 km of conductor have been manufactured in units longer than 200 m.

In the conductor for the T-15 (10), a flat cable of 11 nonstabilized Nb_3Sn strands (1.5 mm diam) around a bronze strip was bonded after heat treatment to two copper pipes (3 mm inner diameter) by an electroplated Cu layer, 1.2 mm thick; see Fig. 3(b). Some copper wires were included between the cable and the pipes to obtain a more regular envelope. To minimize the bending strain during winding, the heat-treated cable is close to the neutral bending axis of the conductor. In the winding of the T-15 coils, a wet insulation method had to be applied to smooth the uneven conductor surface. Over 100 km of conductor have been manufactured, in units of 200 m.

After the T-7 and T-15 manufacturing experience, the technique of assembly by electroplating was not applied any more. The low process speed, the large electric power requirement, and the poor dimensional tolerance overcame the advantage of a good, low-resistance bonding of the components.

Strands Soldered on a Central Copper Pipe.

The OMEGA Conductor. The conductor for the OMEGA detector at CERN is a historical milestone in the development of forced flow superconductors (11). The development started in 1968, with a prototype consisting of a round-in-square copper pipe with eight multifilamentary strips located in longitudinal slots. The 40 × 40 mm assembly was fed into an outer copper pipe and compacted by drawing to the final size of 18

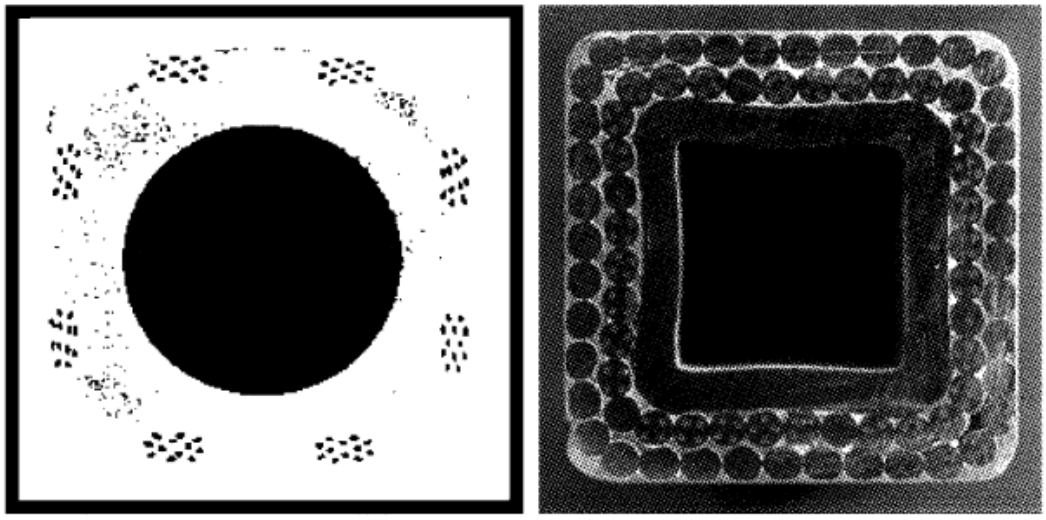

Fig. 4. OMEGA conductor: (a) prototype (left) and (b) final soldered cable. Courtesy of ABB.

$\times$ 18 mm [Fig. 4(a)]. This first approach was abandoned because of the high cost, the limited manufacturing length (40 m), and the lack of transposition.

The final cross section is shown in Fig. 4(b). Manufactured in 1970 at BBC (Switzerland), the 18 $\times$ 18 mm conductor is a square copper pipe with residual resistance ratio (RRR) >250, surrounded by two layers of wires (1.5 mm diam) cabled in opposite directions. In the first layer, 30 out of 36 wires are superconducting, with four NbTi thick filaments (250 μm) in a low RRR copper matrix. The strands are initially not twisted, but, as they are cabled on the copper pipe, no back rotation of the cage strander is allowed, so that the filaments in the strand have the same twist pitch as the cable (200 mm). The second layer, with protective function, contains 40 copper wires and is cabled in the opposite direction, with pitch 180 mm.

The cabled conductor was driven into a SnAg5 bath and pulled through a square die, with a die angle of 45°, cooled at constant temperature to solidify the solder; see Fig. 5. Twelve sections, about 1 km each, were produced for a total of 24 tonnes (11.4 km). The soldering process for each section took about 35 h, at a speed of 0.45 m/min. The online quality assurance included eddy currents and ultrasonics to check the quality of the solder impregnation.

The OMEGA's Brothers. The smallest brother of the OMEGA is a rectangular conductor developed in the early seventies at *ETL*, Japan (7), consisting of a copper pipe with one layer of 52 wires (0.32 mm diam) cabled around and impregnated with SnAg solder. Half of the wires are multifilamentary NbTi strands, alternated to copper wires. In contrast with the OMEGA, the wires are cabled and soldered as a round conductor and later drawn down to the final rectangular size of 5 $\times$ 4 mm; seeFig. 6(a)

In the mid seventies, a conductor of identical size to the OMEGA (18 $\times$ 18 mm) was manufactured at CERN for a large superconducting dipole (12). The copper pipe, with 10 mm bore, is round, and only one layer of NbTi multifilamentary strands and copper wires is cabled on it. The cable is encased between two copper profiles and bonded by SnAg soldering; see Fig. 6(b). The unit length is up to 270 m, and the overall production is more than 5 km.

In the late seventies, a hollow conductor [see Fig. 6(c).] was manufactured at VAC, Germany (13). A loose layer of 20 NbTi multifilamentary strands and 10 copper wires were cabled and soldered in the same process

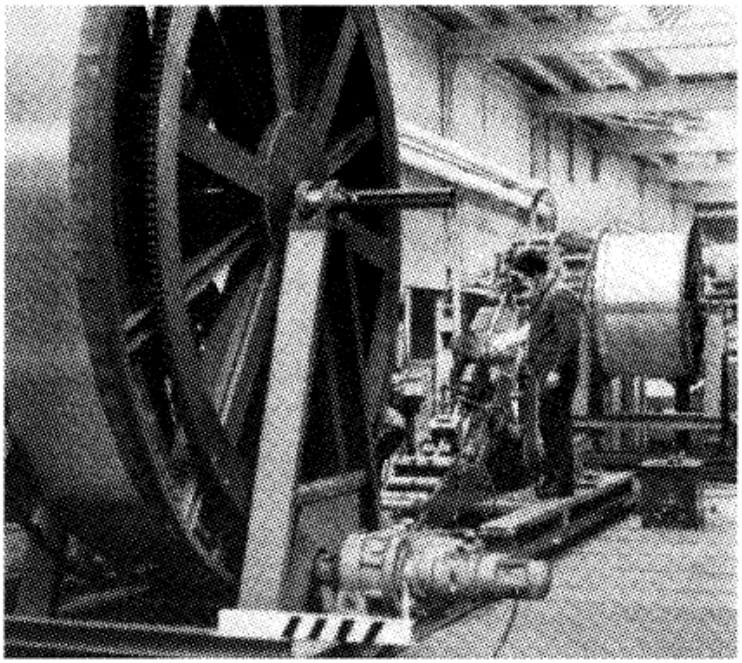

Fig. 5. Soldering of the OMEGA conductor (courtesy of ABB).

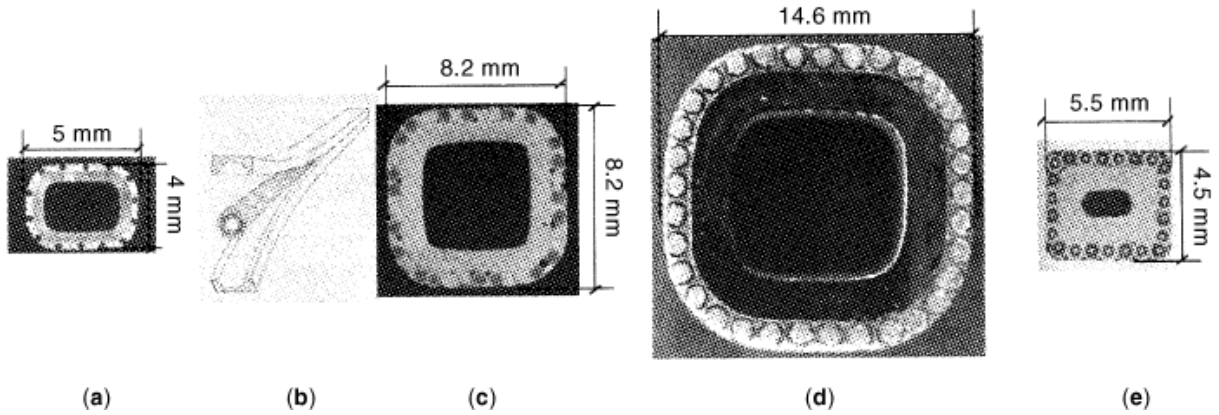

Fig. 6. Soldered, hollow conductors, manufactured similarly to the OMEGA conductor. See text for details.

around a square copper pipe. The solder is SnPb eutectic alloy, and the final size is 8.2 × 8.2 mm. A first conductor batch had to be replaced, as it did not withstand the tight bending radius (over 4% bending strain). About 500 m of conductor was used for the test facility SAFFO at ENEA (formerly CNEN), Italy.

A similar, bigger conductor [see Fig. 6(d)] was manufactured in 1981 at Europa Metalli, Italy (14). The 33 NbTi strands (1.3 mm diam) were first cabled on a round copper pipe and soldered by SnPb alloy. The conductor was then shaped approximately to a rounded square, 14.6 × 14.6 mm. About 9 km of conductor have been manufactured and wound into the outer module of the SULTAN test facility (Villigen, Switzerland).

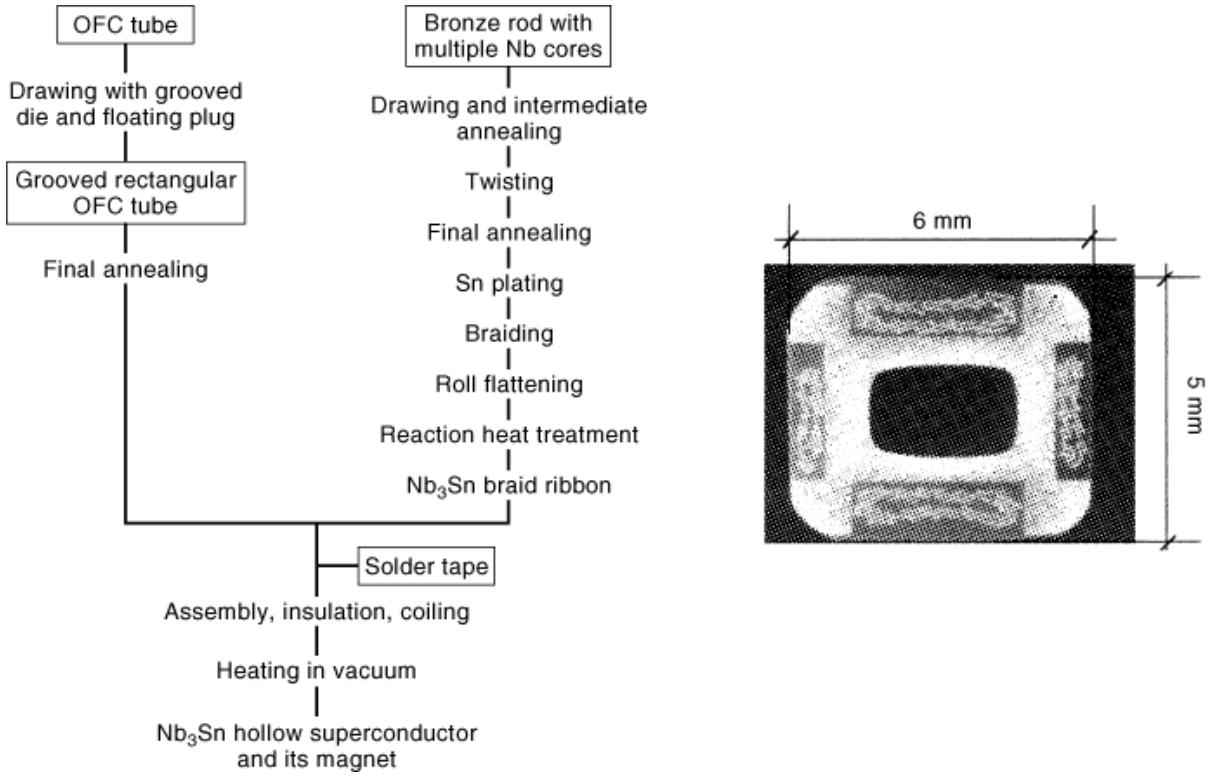

Fig. 7. Nb_3 Sn hollow conductor, with four braids soldered in the slots of the Cu pipe (16), according to the react, wind, and solder process (courtesy of K. Agatsuma, *ETL*, Japan).

Another little brother of the OMEGA [see Fig. 6(e)] has been manufactured at BBC in 1981, for a Sector Cyclotron, SuSe (15), in Munich, Germany. The rectangular copper pipe has a tiny hole, 1×2 mm. Two kinds of NbTi strands, with 0.7 mm diameter and different Cu: non-Cu ratios, were cabled around the copper pipe and soldered with SnAg alloy. The overall conductor size is 4.5×5.5 mm. About 4.5 km of conductor has been wound into the winding of the sector cyclotron, with a minimum bending radius of 68 mm (3.3% bending strain).

The Nb_3Sn Hollow Conductor at ETL, Japan. Apparently, the method of cabling and soldering the superconducting strands on a copper pipe does not apply to Nb_3 Sn conductors: soldering must be carried out after heat treatment, but a heat-treated strand cannot be cabled because of its brittleness. Agatsuma et al. (16) reported in 1978 an ingenious method to prepare a Nb_3Sn conductor soldered on a copper pipe, according to the steps in Fig. 7. called the "react, wind, and solder" method.

Initially, two round, hollow braids (12 and 24 strands) are made from thin, Sn-plated Nb–bronze composites (0.1 mm diam). The hollow braids are flattened to a $\approx$0.6 mm thick ribbon, wound on a large-diameter holder, and heat treated to form the Nb_3Sn composite. In a single process, two small and two large braids are driven, together with a SnAg solder foil, into longitudinal slots on a rectangular copper pipe. The conductor, wrapped with a polyimide film and a reinforcing steel tape, is wound into a coil with 75 mm minimum bending radius. After winding, the coil is heated in vacuum to melt the solder and bond the braids to the copper pipe; see Fig. 7.

If the conductor were a solid monolith during the winding process, the bending strain at the Nb_3Sn filaments would be in excess of 3%, which would be fatal for the conductor (to avoid irreversible damage in Nb_3Sn, the bending strain should be below $\pm 0.5\%$). However, as the braids have not yet been bonded to the copper pipe, the strands can settle in the slots and the actual bending strain is much smaller. A length of 160 m conductor was used for the test coil, which was successfully tested, demonstrating the viability of the process.

The strands in the braids are transposed, but not the four braids placed in the longitudinal slots. To obtain a high-current conductor, a very large number of thin strands must be braided. The conductor layout, with thin braids placed on the perimeter of the pipe, does not allow a large operating current density. Since the successful demonstration, no further application of the process has been reported.

The Swiss LCT Conductor. The most complex conductor belonging to the OMEGA family is the Swiss LCT conductor, manufactured in 1981–1983 at BBC for the Swiss contribution to the Large Coil Task at Oak Ridge. Initially, two forced flow conductor layouts were developed, one being a two-stage cable in conduit and the other a multistage soldered cable around a copper pipe (17). The reasons to prefer the second option were mostly the cost and the slowness of the first. Today, this choice may sound surprising and the same reasons would rather lead us to prefer the cable-in-conduit option. However, in 1981 BBC had developed a broad knowhow on soldered conductors, and almost no industrial experience was available on welding of long lengths of steel conduit.

The cable layout is summarized in Fig. 8. The first cable stage consists of 10 multifilamentary NbTi strands (0.46 mm diam) cabled around a copper wire and solder-impregnated. To limit the ac losses, the first cable stage is tightly wrapped with a 0.05 mm thick CuNi strip and soldered again to bond the wrap to the cable. To maintain full transposition, the second cable stage is made of six subcables around a thick copper core (2.25 mm diam). Eight second cable stages are eventually cabled with the tight pitch of 150 mm around a round copper pipe (7.5×4.5 mm), wrapped with CuNi foil. The cable is compacted and shaped by rolls to a square of 18.5×18.5 mm. Despite the large load required to compact the rigid, solder-impregnated components down to a local void fraction of 30%, neither damage nor performance degradation was observed in the compacted cable.

For the final solder filling of the multistage cable, a special CdZnAg alloy was selected (18), with superior mechanical properties to those of PbSn and SnAg alloys. As the melting point of the solder is about 350°C, the process speed had to be maintained in the range of 2 m/min to avoid degradation of the NbTi critical current density. Due to the high speed, the die needed to be specially laid out. To prevent solder oxidization and for environmental reasons (Cd vapor), the process was carried out under nitrogen atmosphere. The overall length produced for the Swiss LCT conductor was ≈ 5.5 km, in units of 250 m.

The Swiss LCT conductor marked the end of a successful series of hollow conductors cabled and soldered around a copper pipe. As in the OMEGA and its brothers, a single-stage cable was used, so the achievable current density was low, because only one layer of strands could be placed on the outer perimeter of the pipe. The option to use a multistage cable around the pipe was viable, but turned out to have drawbacks: the solder cross section climbed above 25%, and complex, high-resistivity barriers had to be included to avoid large coupling-current losses.

Flat Cables Soldered to Copper Pipes. In Nb_3 Sn react-and-wind conductors, the serconducting strands must stay as close as possible to the neutral bending axis to avoid substantial strain-induced degradation during winding. This requirement, together with the wish to maintain the advantages of the copper pipes, drove in the eighties the development of a number of flat cables assembled by soldering to copper pipes. The ECN (The Netherlands) and the SIN (later CRPP, Switzerland) carried out the conductor development and manufacture as part of the construction of the SULTAN test facility.

The smallest of this conductor subgroup is a NbTi-based flat cable soldered to the broad side of a rectangular, half-hard copper pipe to build a square conductor, 8.4×8.4 mm; see Fig. 9(a). The cable is made by 16 multifilamentary strands with 75 mm pitch and is not at the neutral bending axis, but this is not crucial for the ductile NbTi conductor: the bending strain in the winding is smaller than 1%. The soldering process

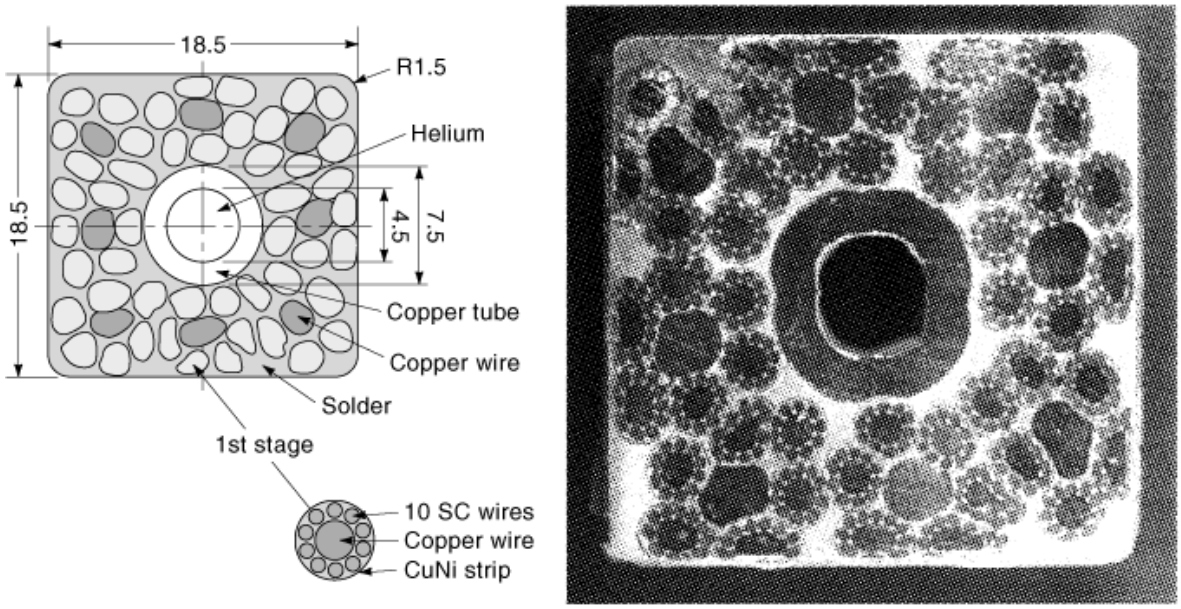

Fig. 8. The Swiss LCT conductor. Dimensions in millimeters. (Courtesy of ABB).

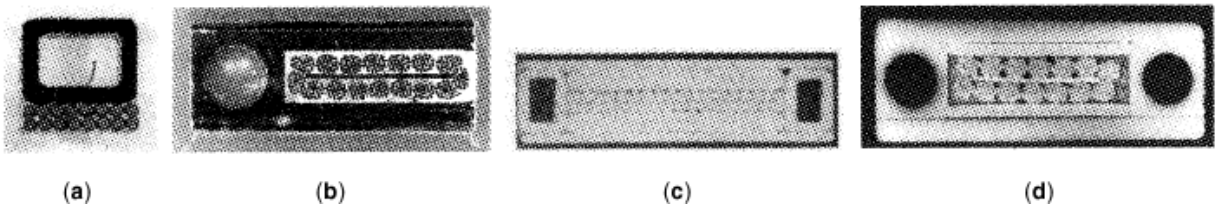

Fig. 9. Flat cables soldered to copper pipes: (a) NbTi ECN 8 T, 8.4 × 8.4 mm; (b) Nb_3 Sn SIN 12 T, 21.5 × 8.4; (c) Nb_3 Sn ECN 12 T, 26.2 × 7.0 mm; (d) Nb_3 Sn SIN 9 T, 26.3 × 9.6 mm. (Courtesy of the SULTAN group.)

was carried out at MCA, Massachusetts, in 1982 (19). A wave soldering device was not sufficient to fill the interstices satisfactorily and had to be modified by adding a restraining die, where the solder becomes solid, as in the OMEGA process. The solder cross section is less than 5%. Ten sections have been produced, each 500 m long.

The Nb_3Sn react-and-wind conductor in Fig. 9(b) was manufactured at SIN (later CRPP) in 1985 (20). The flat cable is made of 2016 multifilamentary strands (0.125 mm diam) according to the external Sn method. The first cable stage (not fully transposed) is composed of 7 strands (1 + 6). The second cable stage (also nontransposed) is composed of two layers of strands (6 + 12) cabled around a copper core. The last stage is a 970 m long flat cable (3.3 × 13.8 mm) of 16 subcables around a bronze strip. The flat cable is heat-treated on an Inconel drum (7 layers) at a radius of 600 mm. This allows straightening the cable after heat treatment without irreversible damage of the Nb_3Sn filaments and bending it eventually to the minimum winding radius, ≈300 mm, with the tolerable bending strain of ±0.28% in Nb_3Sn.

The other components to be attached to the flat cable are a copper pipe, a copper profile as stabilizer, and two stainless steel strips as a structural reinforcement. These four parts have been assembled with three brazing foils and brazed at 630°C for a total length of 930 m in a continuous process, at the rate of 0.3 m/min.

The process could be stopped and restarted to replace the heating elements. The 200 m long sections of the copper pipe were preliminarily brazed to a full length, using a higher-melting alloy.

The brazed steel–copper composite and the heat-treated Nb_3Sn cable were assembled in a combined continuous milling–soldering process. A slot is milled in the copper strip, and the cable is carefully placed in the slot. Bonding of the cable to the copper is achieved by a wave soldering device: the PbSn alloy fills up to 80% of the void area in the cable. The process speed is 0.5 m/min. Stop and restart was necessary every 70 m to replace the cutting tool. As the thickness of the heat-treated cable varied at the layer transition, the thickness of the slot had to be periodically adjusted. The 21.5 $\times$ 8.4 mm conductor was produced in a single length of 870 m and wound into a solenoid. The coil performance confirmed that, besides the expected bending strain, no significant degradation occurred during the manufacturing process. The dc-operated coil did not suffer from the lack of transposition in the cable.

For the Nb_3Sn conductor manufactured in 1986 at ECN (The Netherlands), see Fig. 9(c), some features have been simplified (21). The flat cable, 18.5 $\times$ 1.85 mm, is made of 36 multifilamentary strands (1 mm diam, powder-in-tube method), without central strip. The seven cable sections, about 140 m long, are wound as loose pancakes on steel supports and heat-treated. The other conductor components (two steel strips, two copper pipes, and two copper strips) are all assembled to the heat-treated cable in one run by a wave soldering device. The steel strips were preliminarily electroplated with solder to ease the bonding. The process speed was 1 m/min. Six out of seven conductor sections (total about 800 m) were wound as double pancakes with interpancake joints.

To complete the SULTAN test facility in the split-coil configuration, three additional conductor lengths were manufactured at SIN in 1988 and 1990; see Fig. 9(d). (22). The flat cable, 13.7 $\times$ 3.54 mm, is made of 98 multifilamentary strands (0.65 mm diam, bronze method), cabled in two stages, $(1 + 6) \times 14$, around a central bronze strip. After heat treatment, the components are assembled in a single run (See Fig. 10), as in the ECN conductor, by a wave soldering device, at the rate of 0.3 m/min. Two conductor lengths, 27.0 $\times$ 10.3 mm, each $\approx$ 800 m long, were wound into the two 9 T coils of the SULTAN facility. A third conductor section, 26.1 $\times$ 7.6 mm, 800 m long, with thinner steel strips, was used for the innermost, 12 T coils.

Sheathed Flat Cables

The first attempts to place the active superconducting elements inside a hydraulic conduit date back to the late seventies. Besides the group of bundle conductors (see below), a small number of conductors have been developed by encasing a more or less rigid flat cable into a welded conduit.

The EU-LCT Conductor. Vacuumschmelze (Germany) manufactured the EU-LCT conductor in 1980–1981 (23) after three years of development (24). The design optimization effort (ac loss, stability, and structural aspects) led to a sophisticated conductor layout, requiring four continuous manufacturing processes to assemble the components at very tight tolerance. The single-stage, NbTi flat cable, (stainless-steel-sheathed, 40 $\times$ 10 mm) is shown in Fig. 11.

Twenty-three NbTi rectangular composites, 2.35 $\times$ 3.1 mm, are cabled and soldered on a flat core, which has a central insulating foil to avoid large interstrand coupling-current losses. The core is prepared starting from a NiCr 0.5 mm thick strip, clad on one side with a 50 μm thick CuNi layer to provide a base for soldering. A 4 μm thick Sn coating is electroplated on the CuNi side of the strip. The strip is folded on a 50 μm thick Kapton foil to form the core of the cable. To improve the strength, the folded strip is stretched, adding 6% cold work. The tolerance on the final size of the strip is $(33.8 \pm 0.55) \times (1.0 \pm 0.03)$ mm. Two foils of SnPbIn solder, 50 μm thick, are then attached to the strip by fusing at both edges. The rate of the process is 5 m/min.

A cage strander with full back twist is used to wind the 23 composites edgewise on the flat strip, without adding torsion to the bending. A Roebel head at the cabling point bends the composites accurately at the edge of the flat core, always maintaining the short side of the composite parallel to the flat core; see Fig. 11. Spacing

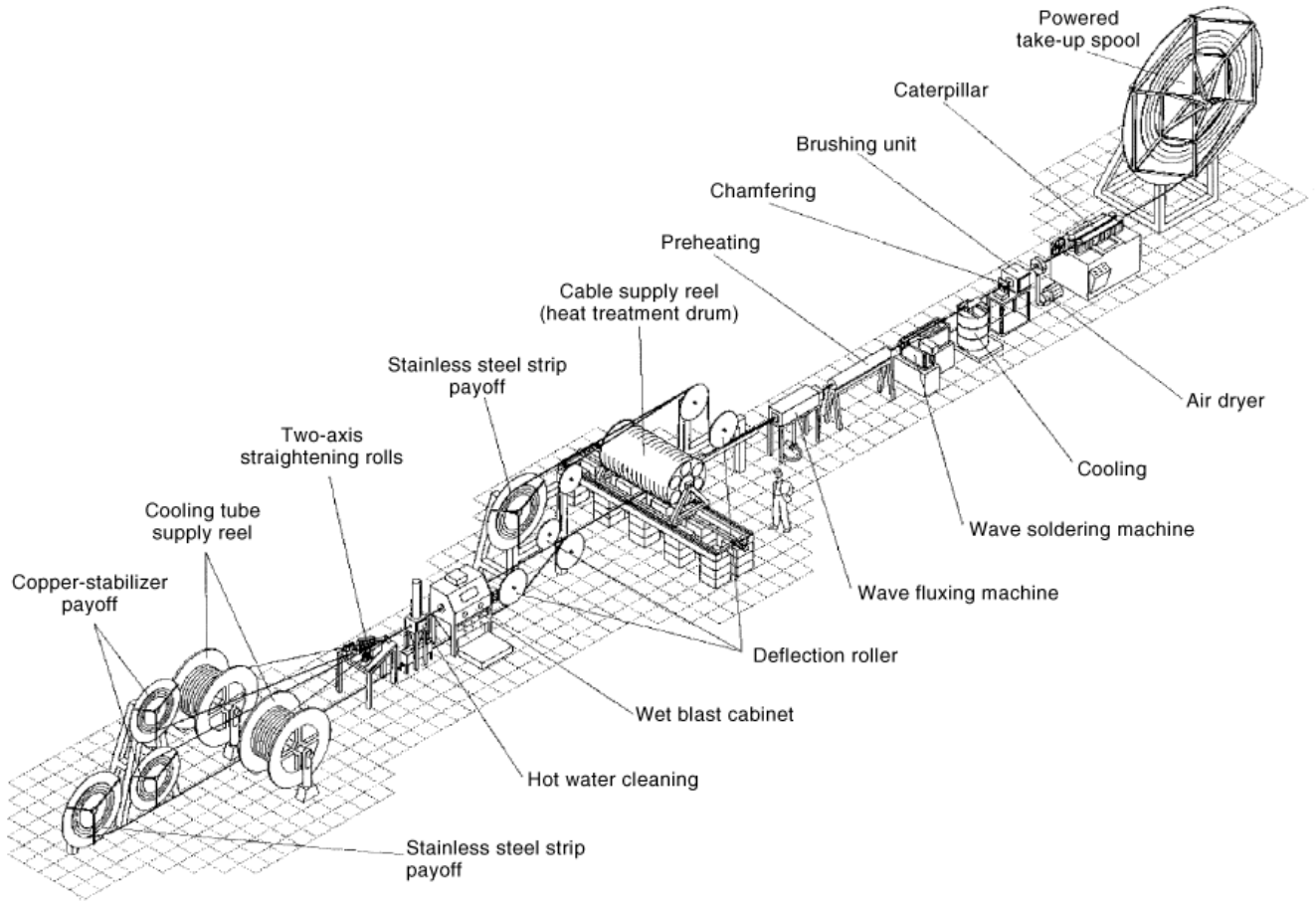

Fig. 10. The milling–soldering line for the final assembly of the Nb_3 Sn react-and-wind conductor for SULTAN (courtesy of G. Pasztor, CRPP).

wires cabled together with the superconducting composites keep the 0.8 mm space between the strands. In the same process, the strands are bonded to the core by melting the solder foils. This is achieved by pressing hot metal blocks on the cable: the strand temperature is 200° to 210°C for about 10 s. The load is maintained till full solidification occurs. Afterwards, the NiCr spacing wires, coated with a refractory varnish, are removed. The transposition pitch is long (400 mm); however, the interstrand coupling-current loss is small, as the strands are electrically in contact only through the thin solder layer. The speed of the cabling–soldering process (See Fig. 12) is 1 m/min.

The 0.8 mm thick sheath is a folded strip of nitrogen-alloyed austenitic steel (316LN). To create additional cooling channels and to limit the heat load to the superconductor during the welding, six steel spacers, 0.6 mm thick, are placed between the cable and the sheath; see Fig. 11. The six spacers are preliminarily attached to the 98 $\times$ 0.8 mm strip in a continuous process, by spot electron beam welding, with minimum heat load to the thin strip. To avoid excessive outgasing in the vacuum environment of the electron beam, the steel for the spacers is 316Ti (not nitrogen-alloyed).

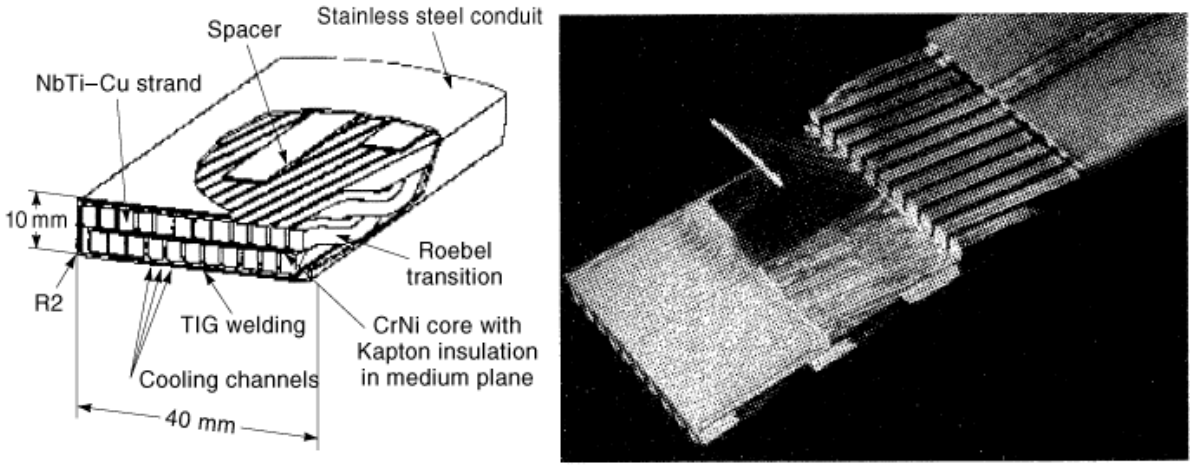

Fig. 11. The EU-LCT conductor (courtesy of Vacuumschmelze, Germany).

The cable sheathing is the fourth and last continuous process for the conductor assembly; see Fig. 12. Six shaping rollers fold the ribbed strip into a U where the cable is fitted, and another six rolls fold the strip around the cable, leaving a welding gap <0.1 mm. A tungsten inert gas (*TIG*) pulsating torch carries out the closing weld. The strand temperature underneath the weld increases to 260°C during 5 s; the temperature rise does not affect the NbTi critical current density. Due to the electrode replacement, the process needed to be interrupted every 50 m. The welding parameters at the restart points are adjusted to guarantee a reliably tight weld transition.

The final tolerance on the conductor size is ±0.1 mm. The corner radius is 2 mm. The conductor has been produced in units of about 500 m, for a total length of 7 km.

Nb_3 Sn Sheathed Flat Cables. The flat cable geometry is attractive for the Nb_3 Sn react-and-wind method because the active, strain-sensitive superconductor can be placed, after the heat treatment, on the neutral bending axis, allowing the conductor to be wound into a coil with minimum degradation. Several such developments were started in Europe and Japan in the eighties, but only few led to significant manufacturing applications.

The three prototype conductors, developed in the mid eighties for the initial phase of the Next European Torus (*NET*) project, were eventually manufactured only in ≈ 10 m sections (25,26,27). The rectangular conductors include a heat-treated Nb_3Sn flat cable, 4.0 to 6.6 mm thick. An insulating core in the center of the cable to reduce the coupling loss was shown not to be necessary (27), so the cable thickness could be reduced. The stabilizer, assembled either as a mixed matrix monolith or as a transposed cable, is soldered to both sides of the flat cable. The conduit is assembled around the soldered conductor by welding four steel strips. The cooling channels are placed underneath the full-penetration weld seams: a strip folding process is not allowed, due to the required conduit thickness (2.5 to 3.2 mm). Laser beam welding was needed to reduce the heat load to the soft soldered cable and to maintain the tight assembly tolerance.

A Russian prototype react-and-wind conductor (28) has a layout similar to the NET prototypes, with four stainless steel strips welded to form the outer sheath. However, the helium channels are eight parallel copper pipes soldered to the central Nb_3Sn flat cable, and the weld seams do not need to be helium-tight.

The ETL Wind-and-React Flat Conductor. An unusual example of a Nb_3Sn flat cable-in-conduit, wind-and-react conductor was developed in the early eighties at *ETL*, Japan (29). Two coreless flat cables, each made of 15 stabilized Nb_3Sn strands 1.4 mm in diameter, are separated by a CuNi strip to reduce the coupling loss (lack of transposition). Two thick copper strips are rolled to form ribbed, U-shaped profiles with large

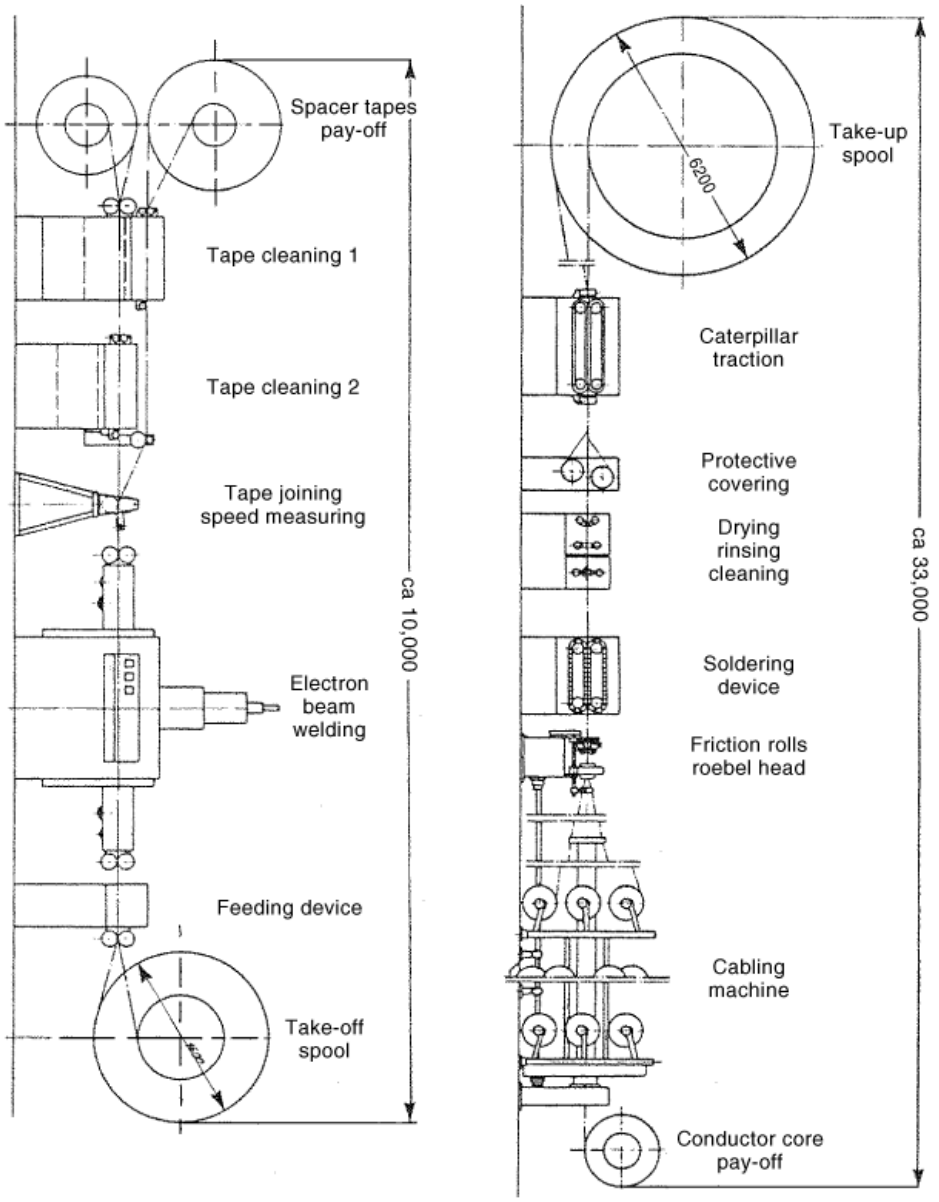

Fig. 12. The cabling–soldering (upper) and the sheathing (lower) processes for the EU-LCT conductor (courtesy of Vacuumschmelze, Germany).

cooling channels for the helium flow (the coolant is also allowed to flow in the interstices between cables and stabilizers). The cable sandwich is assembled with the copper stabilizer and wrapped with a punched CuNi tape: the components are not bonded together. The 0.75 mm thick outer copper sheath is welded in a tube mill. The wrapped cable–stabilizer is pulled through the welded copper pipe and drawn down to the final dimension

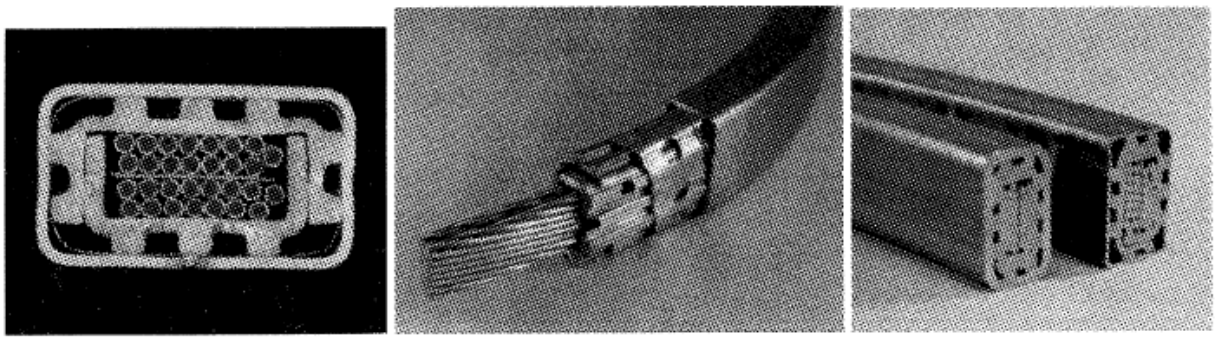

Fig. 13. The 13 × 23 mm Nb_3 Sn wind-react conductor developed at *ETL*: coppersheathed, conductors, left and middle; stainless-steel-sheathed conductors, right (courtesy of K.Agatsuma, *ETL*. Japan).

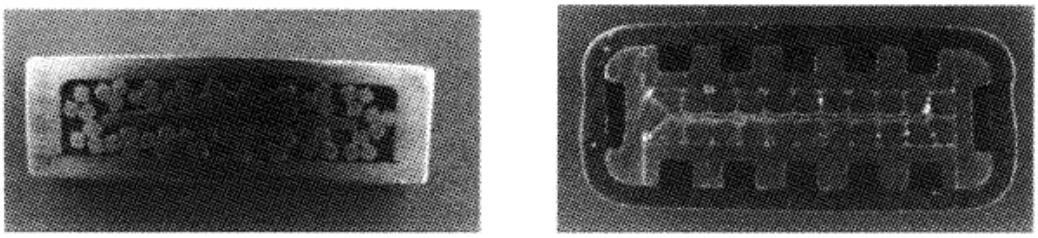

Fig. 14. React-and-wind Nb_3 Sn conductors developed at JAERI for toroidal field coils: (a) STEP-1, and (b) TMC-FF (courtesy of JAERI, Naka).

of 13 × 23 mm; see Fig. 13.. After the die, the conductor passes through a high-frequency annealing furnace to soften the sheath. The production unit length (≈ 40 m) is limited by the size of the drawing bench.

Eight conductor sections (total about 300 m) were insulated by glass tape, wound into a coil with 300 mm inner diameter (over 4% bending strain) and eventually heat-treated to form the Nb_3Sn.

The same manufacturing process was also applied for a stainless-steel-sheathed conductor (30). The selected steel was 316L, the wall thickness 0.6 mm. Wrinkling of the sheath was observed at the smallest winding radius. The properties of the longitudinal *TIG* welding seam were investigated before and after heat treatment (800°C, 50 h). A pancake coil was wound, heat-treated, and tested with eight other pancakes based on Cu-sheathed conductors. The busbars for the coil are manufactured with a thicker (1.5 mm) steel sheath; see Fig. 13.

The TMC-FF Conductor at JAERI. The development of Nb_3 Sn flat cable, react-and-wind conductors for toroidal field coils started at JAERI in the early eighties with a short prototype, called STEP-1 (31); see Fig. 14(a). A Nb layer was included at the outer surface of the strand as a thermal barrier, to delay the diffusion inside the strand of heat from friction at the strand surface. Eventually, the strand was drawn through a star-shaped die cutting four grooves in the Nb outer shell to allow heat exchange between coolant and stabilizer. The sheath was planned to be a thin CuNi strip with an outer steel reinforcement. However, the short prototype was jacketed in a steel U profile with a welded lid.

The actual toroidal model pancake was wound in 1991 with 90 m of monolithic flat cable manufactured by Hitachi Cable 32; see Fig. 14(b). The 4.8 mm thick Nb_3Sn cable consists of 23 nonstabilized strands soldered after heat treatment to a number of U-shaped copper profiles, to build a monolithic, ribbed assembly. To

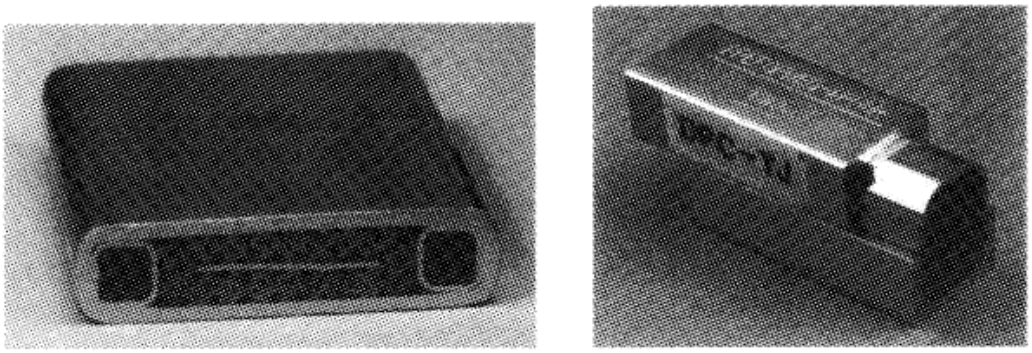

Fig. 15. React-and-wind poloidal Nb_3 Sn conductors developed at JAERI: (a) the *DPC*-EX, 10.2 × 40.8 mm; (b) the *DPC*-TJ with the steel shell machined reinforcement welded longitudinally around the thin conduit. (Courtesy of JAERI, Naka.)

increase the loop resistance and lessen coupling-current losses, a few epoxy spacers are interleaved between the stabilizer elements. It was planned to build the conduit by longitudinal welding of two hot-rolled, 3 mm thick steel profiles to obtain sharp outer corners and improve the conductor's rigidity. However, this development was skipped, and the conduit for the 90 m model conductor was a 2 mm thick steel sheath, *TIG*-welded in a tube mill process.

The DPC-EX Conductor at JAERI. The Nb_3Sn conductor for the Demonstration Poloidal Coil (*DPC*-EX coil) was manufactured in 1988–89 at Mitsubishi Electric (33); see Fig. 15. Over 500 m of the 10.2 × 40.8 mm conductor have been produced in two sections and wound after heat treatment into two double pancakes. From the design point of view, the *DPC*-EX represents the transition between the generation of the flat hollow conductors and the emerging group of bundle conductors (rope-in-pipe or cable-in-conduit).

The 153 Cr plated strands (0.81 mm diam) are cabled in three stages, 3 × 3 × 17. The last cable stage has a steel strip core to cut the interstrand coupling loss. The helium void fraction in the cable space is in excess of 40%. At both sides of the cable, two stainless steel squared pipes provide the main cooling channels. The helium in the cable space is quasistagnant: every 0.3 m, the steel pipes have *mixing holes* (3 mm diam) to improve the heat exchange with the cable and to avoid a large pressure rise in case of quench. The outer sheath and the two pipes are made of a stainless steel (JK-1) specially developed (34) to maintain high strength and ductility at low temperature after the Nb_3Sn heat treatment at 700°C, 30 h. The conduit has constant thickness, 1.5 mm, and is assembled from two strips, folded and welded by two simultaneous *TIG* seams at the edge side, in a modified tube mill (the steel pipes underneath the seams allow achieving full penetration without damaging the strands).

Cable-In-Conduit Conductors

The development of cable-in-conduit conductors (*CICCs*) started slowly in the late seventies, with only few significant applications till the late eighties. However, as soon as the manufacturing methods had been mastered by the industry, the *CICCs* became very popular, and today they dominate the restricted market for forced flow superconductors. The main design motivation for introducing the cable-in-conduit conductor is its large wetted perimeter, improving the heat exchange and stability for pulsed field applications. The initial development was aimed at Nb_3Sn react-and-wind technology. In the nineties, the use of *CICCs* was extended to the wind-and-react method, as well as to the NbTi technology.

Investigations of the stability and ac loss performance of the *CICCs* stimulated a number of experiments with short-length, small-size conductors manufactured on purpose. This was in contrast with the former forced flow conductors, where the experiments were carried out only on full-size conductors, manufactured to wind a real magnet. The short conductors for small-scale experiments are ignored in this review, as they are mostly irrelevant for the issue of manufacturing methods.

Instead of a one-by-one description of each conductor, the manufacturing aspects are grouped into four categories, with cross-references that cannot always reflect the historical sequence.

Strand Coating. A coating of the strand surface may be applied to control the transverse resistance of the cable as well as the friction and bonding at the strand contact points. The choice of coatings is broad, ranging from the bare strand surface (no coating) to insulating varnish. The design criteria for ac loss and stability (interstrand current sharing) drive the selection of the strand coating; see also the article HYSTERESIS AND COUPLING LOSSES IN SUPERCONDUCTORS. The coating options for Nb_3Sn strands are restricted by the requirement of withstanding the heat treatment.

The properties of metallic coatings for NbTi strands have been thoroughly investigated for accelerator cables (not forced flow conductors). The coating methods include galvanic deposition of Ni, Cr, and Zn, as well as dipping in molten SnAg alloy (35,36). For NbTi-based *CICCs*, copper oxide has been used as a strand surface treatment in a SMES coil (37), and Cr plating for a prototype SMES conductor (38). The bare copper surface has been selected for the dc-operated poloidal coils of the Large Helical Device (39), as well as for a 100 kA conductor of a flux pump (40). Organic-varnish-insulated strands have been used for the CICC of the *DPC*-U coils (41). In the NbTi CICC for the 45 T hybrid magnet (42), the drawing lubricant is intentionally not removed from the strands to enhance the contact resistance. The bare copper surface, as well as the oxidized copper surface, proved to be not satisfactory for pulsed operation (because of high interstrand coupling loss). Conductors with fully insulated strands showed severe instabilities due to their inability to redistribute the current among the strands.

In Nb_3Sn-based *CICCs*, an antibonding coating is highly recommended to avoid intermetallic diffusion at the strand crossovers during heat treatment. If the strands bond together without possibility of sliding during the winding process (react-and-wind), the performance degradation due to the bending strain and the interstrand coupling loss may become unacceptably high. An example of noncoated Nb_3Sn in a CICC, with very high coupling-current losses, is provided by the *DPC*-TJ coil (43).

A 5 μm copper sulfide layer was originally specified, but eventually not applied, for the Westinghouse–LCT conductor (44). The antibonding properties of the copper sulfide have also been assessed in the JA development for Nb_3Sn CICC (45). In the US-*DPC* conductor,some lubricant was accidentally used during the cabling, providing an oil film on the Crcoating (46) Based on this experience and on special ac loss experiments (47), the bare Nb_3Sn strands of the CICC for the 45 T hybrid magnet were intentionally coated with Mobil 1 oil; during the heat treatment the organic film partly vaporizes, leaving a blackened strand surface. The organic vapors may have a detrimental effect on the other conductor components during the heat treatment, and the loose carbonized particles may affect the flow dynamics in operation.

The Cr Electroplating. Today, the large majority of Nb_3Sn strands for *CICCs* are Cr-coated in a continuous electroplating process. The plating of wire with Cr is not a standard process, and a number of new plating lines have been set up, especially for Nb_3Sn strands. Because of the environmental issues associated with Cr electrolyte, the plating lines are mostly assembled at Cr plating companies rather than at companies for continuous galvanic coating of wires.

Compared to other galvanic processes (e.g., Cu, Sn, and Ni), Cr electroplating is much slower (and more expensive too): at a current density of 50 A/dm^2, the growth rate of the Cr layer is in the range of 1 μm/min. To obtain reasonable process speed and prevent the Cr plating from becoming bottleneck in strand production, several strands can be pulled in parallel through the same galvanic bath, or the same strand can make multiple passes through the bath. The process speed is obviously inversely proportional to the required thickness of the Cr layer. As the antibonding effect of the Cr plating is due to the surface oxide, a thin coating (in the range of

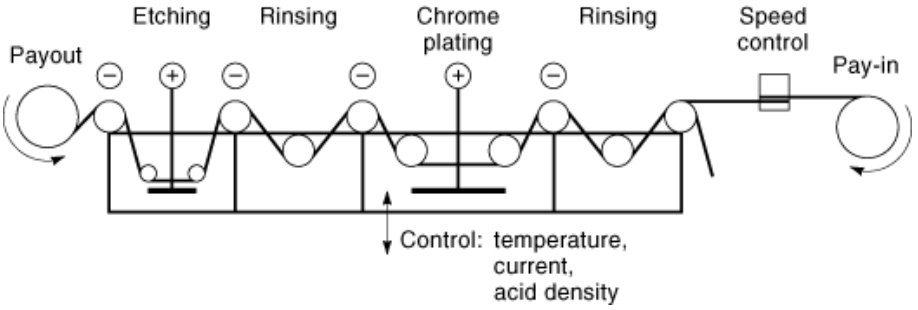

Fig. 16. Scheme of a continuous Cr plating line (courtesy of ABB).

2 μm) is preferable, for cost reasons, to a thicker one. Typical process rates for a 2 μm coating are in the range of 1 m/min for a single pass and can be substantially increased by multiple passes.

Prior to Cr plating, the strand needs to be cleaned, usually by galvanic etching. This step may be either integrated in the Cr plating line (48) (see e.g., Fig. 16) or done separately, together with a surface passivation (49).

The antibonding properties of the Cr plating are well established. However, the contact resistance at the strand crossovers (i.e., the interstrand coupling loss) and the worsening of the copper RRR (due to grain boundary diffusion during the heat treatment) may vary over a broad range, depending on the proprietary electroplating process of the different vendors (50). A discussion of the role of the electrolyte composition is given in Ref. 51.

Strand Bundling. The way of bundling the strands in a CICC may have a crucial effect on the conductor's performance. For an even current distribution under time-varying current operation, the path, and thus the self-inductance, of each strand in the bundle must be identical. This requirement may also be formulated as full transposition with respect to the perpendicular applied field. Layered cables of superconducting strands, for example $1 + 6$ or $1 + 6 + 12$ configurations, should be avoided. However, it is allowed to place a nonsuperconducting core at the center of a cable, as for example in the Swiss LCT cable (17): this option is satisfactory for transposition issues, but further investigations are required to assess the role of the central core ("segregated" copper) as a stabilizer for transient events. Among the coreless stranded bundles, the triplet is definitely the most stable geometry. With increasing number of strands (e.g., five or six) there is a tendency for one strand to slip to the center, making an imperfect, non-fully-transposed, $1 + 4$ or $1 + 5$ cable.

To bundle together a reasonable number of superconducting wires, multiple stranding (multistage cabling) is necessary. To preserve the transposition, the pitches of each cable stage must not be integer multiples. To avoid strand damage (45) and to reduce the interstrand coupling loss (52), the pitch direction must be the same in all the cable stages. The typical pitch lengths are in the range of 10 to 20 times the diameter of the cable stages. A sequence of tight pitches turns into a stiff cable with a large average angle of the strands to the conductor axis, leading to ineffective use of the cross section. On the other hand, a sequence of loose pitches may lead to strand slippage during the bundle compaction, with local transposition errors. The pitch of the last cable stage is crucial for coupling loss. In very large bundles, the subcables may be wrapped with a high-resistivity metal strip to cut the largest coupling-current loops (53). The wrap direction must be opposite to the pitch direction to avoid loosening and crinkling of the strip when cabling the next stage with back twist. The wrap may be spaced (no overlapping) to allow some coolant mass exchange. The use of the subcable wraps to cut the interstrand coupling currents must be carefully watched in the design, as it may lead to a severe penalty in interstrand current sharing and current redistribution.

The selection of the cable stage sequence, especially the number of elements in the last cable stage, is made according to the final cable shape—a rectangle, an annulus with central hole, a square bundle, or the

Table 1. Cable Pattern for Selected Large CICCs

Conductor	Ref.	Strand	Coating	Cable Pattern	Strand Diam (mm)	No. of Strands	Void Fraction (%)	Shape
WH-LCT	44	Nb_3Sn	CuS[a]	3 3 3 3 3 3 3 3 6	0.7	486	32	Square
DPC-TJ	54	Nb_3Sn	Bare	3 3 3 3 3 3 3 3 6	0.67	486	40	Rectangl
LHD-OV	55	NbTi	Bare	3 3 3 3 3 3 3 3 6	0.89	486	38	Rectangl
US-DPC	46	Nb_3Sn	Cr	3 3 3 3 5 3 5	0.78	225	43–38	Square
W7-X	56	NbTi	Bare	3 3 4 3 4 3 4	0.55	192	37	Round
SMES-ISTEC	37	NbTi	CuO	3 3 3 3 3 3 3 3 3 3 4	0.62	972	38	Rectangl
GEM	57	NbTi 1 Cu	Bare	3 3 5 3 5 3 6	0.73	450	37	Round
ITER-MC2	53	Nb_3Sn 1 Cu	Cr	3 3 3 3 4 3 5 3 6	0.81	1080	37	Annulus
ITER-MC1	53	Nb_3Sn	Cr	3 3 4 3 4 3 4 3 6	0.81	1152	37	Annulus
DPC-U	58	NbTi	Insulated	3 3 3 3 3 3 3 3 6	1.1	486	46	Rectangl
45 T hybrid-A	59	Nb_3Sn 1 Cu	Oil	(1 1 6) 3 3 3 5 3 5	0.43	525	39	Rectangl

[a] Specified, but eventually not applied.

like. Table 1 (54,55,56,57,58,59) lists a number of fully transposed cable configurations for large bundles (more than 200 strands).

The natural void fraction of a stranded cable prior to compaction is larger than 50%. However, the typical void fraction required in the cable space is in the range of 30% to 45% (higher void fraction may allow strand movement in operation; lower void fraction may affect the integrity of the strands and limit the stability or the hydraulic performance). Compaction of the strand bundle may be achieved either with a die at the cabling point or with shaped rolls (either freely revolving or engine-driven). For large compaction loads, a die is not recommended, as abrasion may occur at the strand surface and large pulling loads may damage the cable. In large multistage cables, progressive compaction is advisable at each cable stage for an even distribution of the voids and to avoid very high compressive loads at the outermost strands. The springback of the bundle after passing the compacting tool must be allowed for in setting the size of the rolls or die. The cross-section reduction of the bundle is preferably done in one step. A thin, overlapped metal wrapping is sometimes applied after compaction to protect the bundle in the subsequent handling and manufacturing processes. A final calibration–shaping pass may be necessary if tight dimensional tolerance is required.

The hydraulic diameter of a strand bundle with ≈40% void fraction is in the same range as the strand diameter. To reduce the pressure drop, whenever large mass flow rate is required in operation, parallel helium channels, with larger hydraulic diameter, may be attached to the strand bundle. In the *DPC*-EX, the extra channels are two perforated steel pipes assembled at both sides of the flat cable (33). In the US-*DPC*, the four-corner area between the central, wrapped bundle and the outer square conduit provides high-speed helium channels (46).

A practical way to add a pressure-relieving helium channel is to cable the strand bundle as an annulus around a central hole. This also provides a sound, fully transposed layout for the last cable stage. The central hole can be obtained by preshaping the subbundles with rollers (in the last but one cable stage) as wedges and fitting them together in the last cable stage (60). In this way, the subbundles form a vault and the central hole does not need a mechanical support. However, matching the preshaped subbundles correctly requires an accurate, continuous adjustment of the back twist of the individual components. The cabling rate is very low, and only a limited compaction load can be applied after cabling. In the ITER conductors (53) [Fig. 17(d, e)], as well as in the prototype 200 kA SMES (61) [Fig. 17(b)], the QUELL conductor (62) [Fig. 17(c)], and the HT-7U (63) [Fig. 17(f)], the last cable stage is formed on a steel spiral that allows helium exchange between the central hole and the bundle. No preshaping is necessary in the subbundles of the ITER conductor, which are compacted against the spiral core, yielding a homogeneous filling of the annulus.

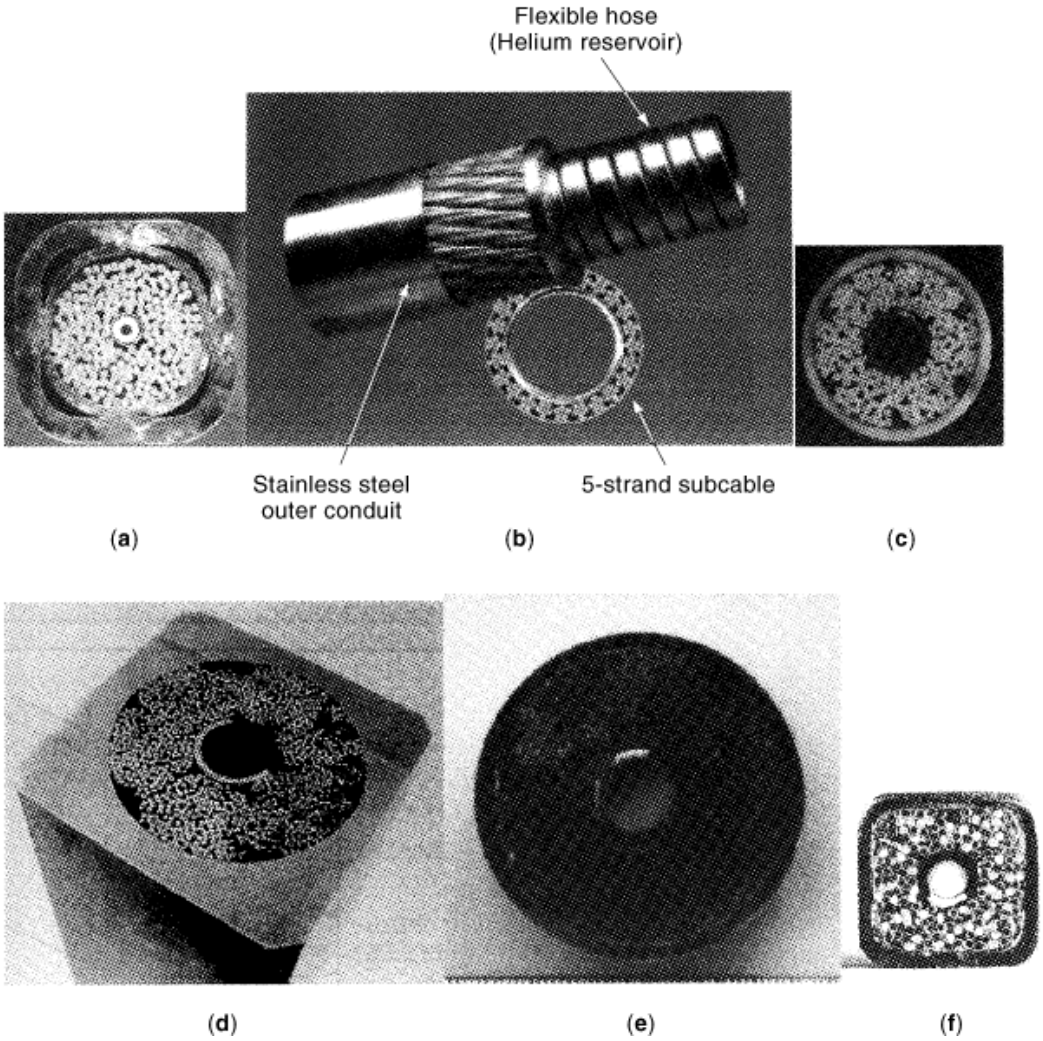

Fig. 17. Examples of CICC with pressure-relieving helium channels: (a) the Nb_3 Sn US-*DPC*, 22.3 × 22.3 mm with central heater (courtesy of MIT); (b) the NbTi 200 kA SMES, 55.1 mm diam (courtesy of Bechtel); (c) the Nb_3 Sn QUELL CICC, 19.4 mm diam (courtesy of CRPP); (d) the Nb_3 Sn ITER-CSMC, 51 × 51 mm (courtesy of ITER); (e) the Nb_3 Al insert conductor, 45.7 mm diam (courtesy of JAERI); (f) the NbTi HT-7U conductor (from Ref. 63).

The subbundles of the Polo conductor (64) are cabled around a solid steel pipe (See Fig. 18), which forms a separate, central conduit for forced flow of two-phase helium at 0.12 MPa. The inner conduit is also wrapped with adhesive layers of Kapton and can be used in the quench detection system to balance the inductive voltage component. The annular space contains stagnant supercritical helium pressurized at 0.4 MPa. The 13 subbundles of six NbTi strands around a CuNi core are spaced by an insulating wrap covering 70% of the surface. Neither instabilities nor ramp rate limitations have been observed in the perfectly transposed conductor, but the dc performance was degraded by 30% (65).

Braided Bundles. Instead of multiple stranding, an alternative way to bundle together the superconducting strands for a CICC is braiding. The hollow braids in common use in electrical engineering (e.g., for

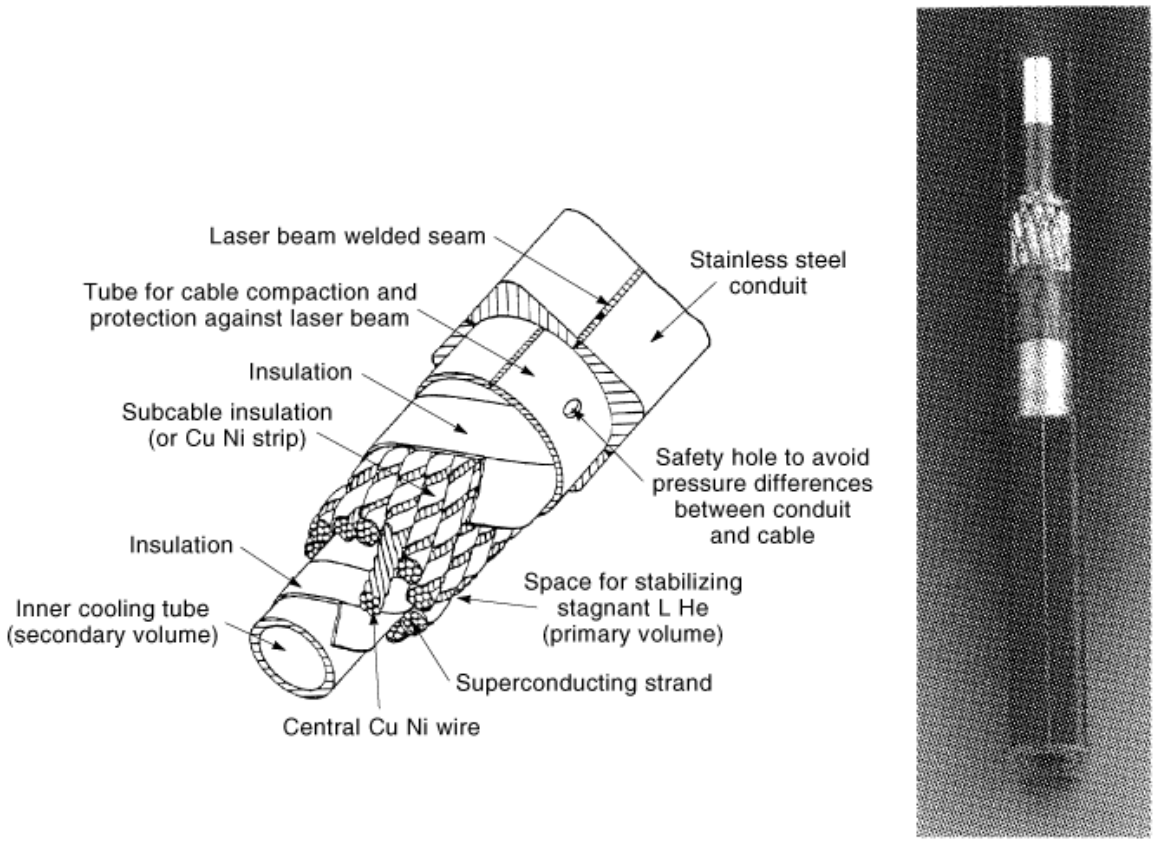

Fig. 18. The Polo conductor, 22.5 × 22.5 mm. with double, separate cooling channels and insulated subbundle (courtesy of VAC).

high-frequency shields) consist of two interlocked multiple spirals with opposite pitch direction. Such hollow braids are transposed for perpendicular field, but are not suitable for a CICC, because the symmetry of the hollow geometry is destroyed during compaction and, in case of parallel time-varying field component, large voltage may be induced between the two opposite by running spirals. The flat braids proposed for superconducting accelerator dipoles are fully transposed for perpendicular and longitudinal applied field, but do not fit, because of the large aspect ratio, into a practical CICC.

In *lattice braids*, similar to some type of alpine ropes, all the elements are interlocked in a bulk bundle. For selected layouts, the strand bundle is fully transposed for both transverse and longitudinal applied field (notice that stranded cables are never transposed for longitudinal applied field). Lattice braids were proposed as an option for the WH-LCT conductor (66). The full transposition, high flexibility, and mechanical stability of the bundle, as well as the large wetted perimeter, made very attractive the idea of a lattice braid as the first cable stage for a CICC bundle. If all the strands are braided at once into a large bundle, the aspect ratio of the braided bundle can be designed starting from the layout of the braiding platform (See Fig. 19) without the need of final shaping as with stranded bundles. The only drawback for practical application of the lattice braids is that such braiding machines are not industrially available and must be specially built. The complexity (and the cost) of the braiding machine sharply increases with the number of elements to the braided at once. For

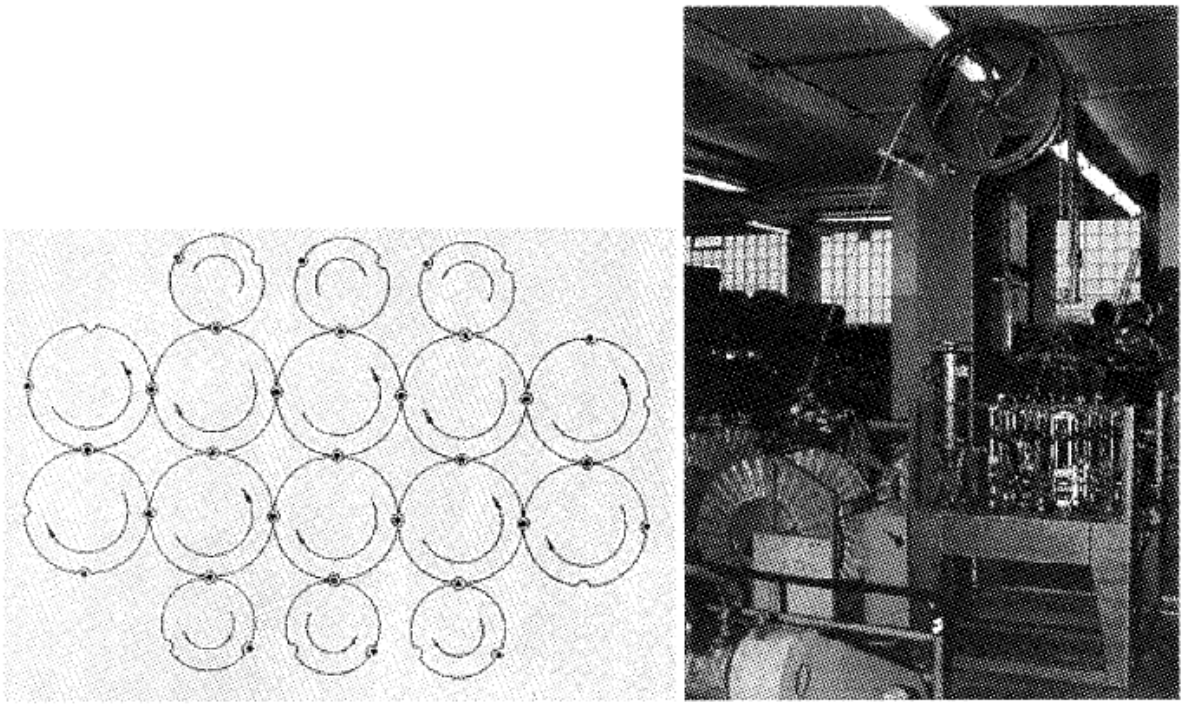

Fig. 19. The 29-strand lattice braid: scheme of the braiding platform with the movements of the carriers (left) and operating braiding machine (right). (Courtesy of ABB.)

this reason, the braid option was abandoned in the WH-LCT, after a few meters of 34-strand bundle had been manually braided.

A powered braiding machine, able to handle 29 strands at once, was built in 1989; see Fig. 19 (48). The 29-strand lattice braid was used as a first cable stage for a rectangular Nb_3Sn prototype CICC (67), with a total of 609 strands ($29 \times 3 \times 7$). Compared to a similar conductor with purely stranded cable configuration ($\times$ 3 $\times$ 3 $\times$ 73 $\times$ 3 $\times$ 3 $\times$ 7) and identical overall void fraction, it is evident from Fig. 20 that the braid-based conductor has a more homogeneous distribution of voids. Mechanical tests (68) also indicate a higher transverse modulus for the braided bundle because of the interlocked structure (no line contacts among strands).

Conduit Materials. The selection of the conduit material is dictated by the mechanical requirement in operation, as well as by manufacturing issues (weldability, industrial availability of strips or pipes, and compatibility with the heat treatment, if any).

Copper is seldom used as a conduit material because of its low strength. The *ETL* wind-and-react Nb_3Sn flat cable (see above) has a 0.75 mm thick, Cu welded sheath (29), manufactured in straight, 40 m long sections by longitudinal welding. A 200 m long section of NbTi CICC with 5×5 strands was manufactured in a continuous tube mill process, using a 0.6 mm thick copper strip (69). Although the coils wound with the copper-sheathed conductors were small (inner radius 0.15 m and 0.26 m respectively), in both cases the sheath cross section was not designed to withstand alone the hoop load in operation.

Low-carbon-content, austenitic steel is the favorite material for CICC sheaths, because of its ductility, strength, broad availability in almost any shape, and low cost. Whenever higher strength is required, nitrogen-alloyed austenitic steels (e.g., AISI 316LN and AISI 304LN) may be used. Some precautions must be taken using the nitrogen-alloyed steels with Nb_3Sn conductors, due to the possible reduction of the fracture toughness after

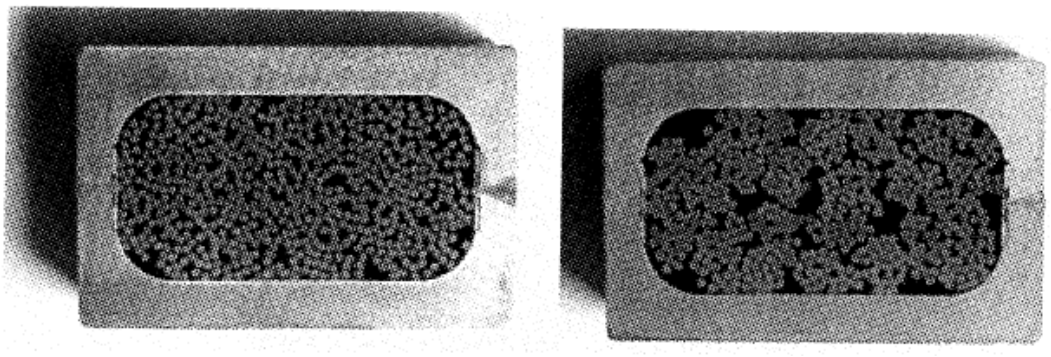

Fig. 20. Cross sections of two prototype *CICCs* for NET: braided bundle, 29 × 3 × 7 (left) and stranded bundle, 3 × 3 × 3 × 3 × 7 (right). (Courtesy of ABB.)

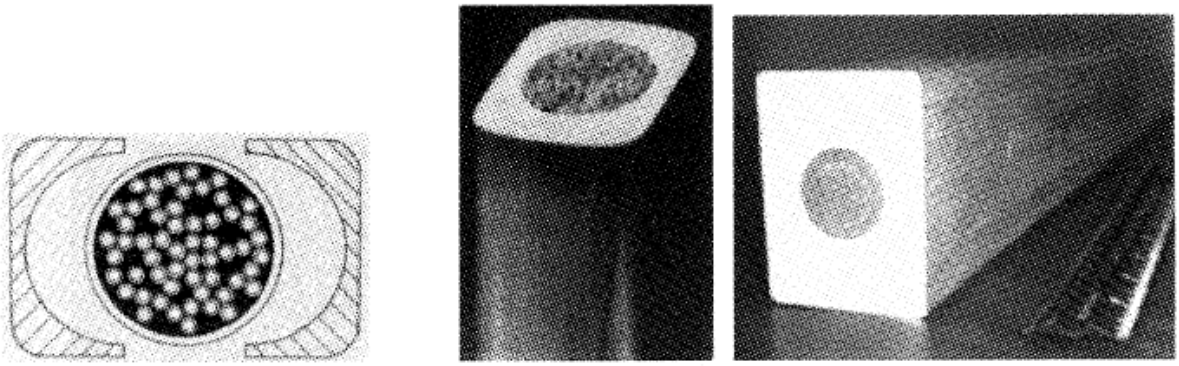

Fig. 21. Use of Al alloys for *CICCs*: (a) an MIT test conductor (courtesy of B. Montgomery) with Al primary conduit and co-wound profiles; (b) the W7-X conductor, with coextruded All6060 alloy (courtesy of EM-LMI); (c) the GEM conductor with steel primary conduit and coextruded outer Al cladding. (Courtesy of N. Martovetsky, LLNL.)

heat treatment. A large effort has been carried out, mostly in Japan, to develop and select suitable stainless steels to prevent degradation of the mechanical properties after heat treatment (70,71,72,73).

Among the relevent Nb_3Sn-based *CICCs* with austenitic steel conduits, we recall the 45 T-A and B hybrid (74), the *DPC*-EX (33), the *DPC*-TJ (54), the ENEA conductor (75), the ITER-TFMC (76), the HFTF (77), the FC 150 m coil (78), and the 12 T TFMC pancake (79).

Most of the NbTi-based *CICCs*, have an austenitic steel conduit, for example, the poloidal LHD coils (55), and the *DPC*-U (58), the EU-LCT (24), the Italian MHD (80), the Polo conductor (64), the 45 T-C hybrid (42), the JF-30 (81), the 200 kA SMES (61), and the HT-7U (63).

Aluminum-Based Conduit. An Al-sheathed CICC [nontransposed cable of 3 × (+ 6 + 121 + 6 + 12) NbTi strands] was manufactured in short lengths in 1977–1978 (82). The 0.9 mm thick Al round pipe, 12 mm diam, was co-wound with two matching Al extruded and anodized profiles; see Fig. 21 The test conductor was bent to small radius and used for stability experiments.

For the W7-X coil system, consisting of nonplanar windings with small bending radius, a NbTi based CICC was proposed (83) with conduit made from a coextruded Al alloy; as extruded, the CICC is soft ($\sigma_y \approx$ 100 MPa) and can be easily bent to small radius. After aging at 130° to 180°C, which can be combined with

the epoxy impregnation process, the Al 6060 alloy hardens ($\sigma_y \approx 280$ MPa at 4 K), providing the required mechanical stiffness to the winding (56). The square conduit, 14.8 × 14.8 mm (See Fig. 21), is coextruded on the 10 mm diam cable, without any protective wrapping, in unit lengths of 600 m. To avoid degradation of the NbTi conductor performance, the temperature and speed of the coextrusion process must be carefully controlled: a decrease by 5.5% of the strand I_c performance was observed for the W7-X conductor (84). The coextrusion of superconducting cables and pure Al is well developed for particle detector magnets. For W7-X, the process was first used to produce an internally cooled conductor.

A coextrusion method was also used for the GEM detector conductor (85). However, here the cable (See Table 1) is preliminarily sheathed with a 1.5 mm thick 304L steel conduit and the thick, pure Al clading has no helium containment function. The bonding of Al to steel was proved to be effective for stability. With an overall size of 49.8 × 68.5 mm (84% consisting of the pure Al clading), the GEM conductor is the largest forced flow conductor manufactured in useful length; see Fig. 21

Incoloy 908 Conduit. The use of a superalloy as a conduit material for CICC was first considered for the Nb_3Sn WH-LCT conductor, due to the disappointing experience after heat treatment with the nitronic 40 (a steel with 0.33% nitrogen content). The R&D work (86) led eventually to the choice of JBK-75, a 30% Ni alloy specially developed from the A-286 superalloy, as a sheath material.

The main drawback of the steel as conduit material for Nb_3Sn *CICCs* is its large coefficient of thermal expansion: from the heat treatment down to the operating temperature, the differential contraction of steel and Nb_3Sn causes a degradation of the superconducting properties, especially severe at high field. In the scope of the US-*DPC* coil R&D program, a new superalloy of the Incoloy group was developed as sheath material for Nb_3Sn *CICCs*, with coefficient of thermal expansion matching that of Nb_3Sn (87). Several test programs have been carried out to compare the mechanical properties of Incoloy 908 and 316 LN steel (see, e.g., Ref. 88). However, the most impressive advantage in the use of Incoloy 908 as a conduit material is the gain in the high-field performance of the Nb_3Sn (89). On the other hand, a big concern in the use of Incoloy 908 is the possible occurrence of *stress-accelerated grain boundary oxidation* (*SAGBO*) during the heat treatment, leading eventually to catastrophic failure of the material. Relaxation of the surface stress in the conduit by shot peening, as well as tight control of the oxygen content (below 1 ppm) in the heat treatment atmosphere, are the key measures to avoid *SAGBO* (90,91).

The US-*DPC* conductor was sheathed with a 2.35 mm thick strip of Incoloy 908, *TIG*-welded in a tube mill (46). The first large-scale application of Incoloy 908 as a conduit material for a Nb_3Sn CICC is ITER-CS model coil conductor (53). Several tens of tonnes of round-in-square tubing, as 6 m to 11 m long sections, have been manufactured by combined hot, hollow extrusion and cold drawing (92).

Pure titanium has been proposed as an alternative low-coefficient-of-thermal-expansion material for sheathing of Nb_3Sn-based *CICCs*. Its low-temperature mechanical properties after aging are reported in Ref. 93. The only important CICC with Ti conduit is the 100 m long QUELL conductor, with 3 × 3 × 4 × 6 Nb_3Sn strands and 1.2 mm thick pure Ti round pipe (62).

Jacketing Methods. The selection of the jacketing method depends to a large extent on the dimension and cross section of the jacket. A key issue affecting the jacketing is the wall thickness. Conduits with constant wall thickness can be manufactured and assembled by a variety of methods, some of which are the cheapest. On the other hand, a conduit with variable wall thickness at the corners allows better packing of the conductor in the winding and offers superior mechanical performance.

The Tube Mill. The large majority of *CICCs* are jacketed by the tube mill method. The generic scheme of the process is shown in Fig. 22, from Ref. 54. The metal strip is formed by rolls around the cable in a large number of steps; see Fig. 23(a) for the WH-LCT conductor (94) Fig. 23(b) for the *DPC*-U (58), and Fig. 23(c) for the 45 T hybrid (59). The longitudinal *TIG* weld is usually done while the conduit is oversize, to limit the thermal load on the strand bundle underneath the welding seam and to avoid contact between the weld bead and the bundle. However, it is also possible to fold the strip exactly to the final size and weld it without damaging the superconductor, as for example in the *DPC*-EX (33) and the EU-LCT (24).

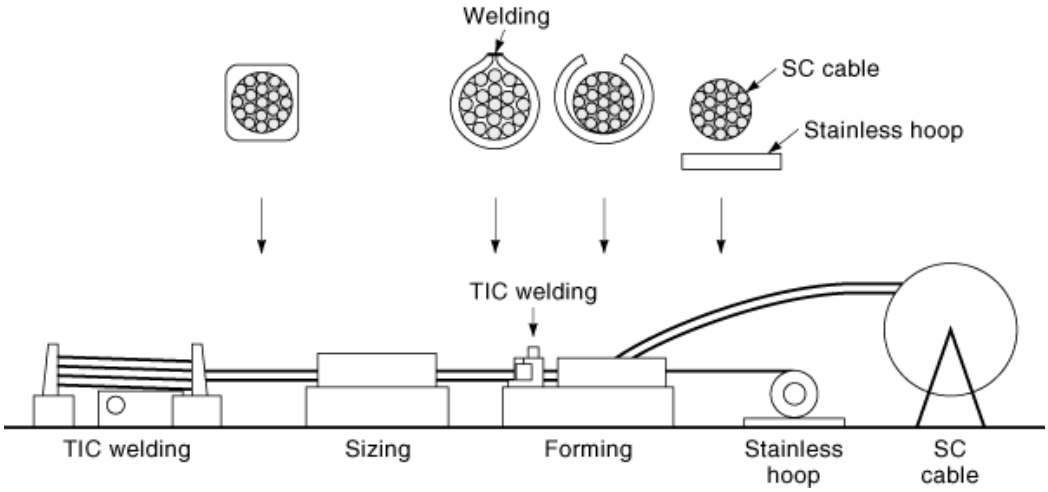

Fig. 22. Scheme of the tube mill method for CICC, courtesy of JAERI.

After forming and welding the round pipe (a highly standardized industrial process), the conduit is compacted in a number of steps to suppress the gap between pipe and bundle, and to give the square or rectangular shape required for winding; see Fig. 23 Typical conduit elongation during the compaction process, by rolling and/or drawing, is up to 10%. It is crucial to control the cable elongation during the compaction: at large cross section reduction and low void fraction, plastic axial deformation of the bundle may start, with fatal consequences for the stranded cable, which does not withstand elongation larger than 2% to 3% without permanent damage. On the other hand, good mechanical engagement between cable and conduit during the final shaping steps is highly desirable, to restrain dangerous strand movements under the operating load.

Starting from a metal strip, it is not possible to achieve sharp corners in the final, squared conductor. The typical range for the outer corner radius is 3 mm to 6 mm, depending on the wall thickness. The final cold work of the conduit (starting from the fully annealed strip) depends on the cross-section reduction, the conduit thickness, and the corner radius.

The thickness of the conduit (typically 1.5 mm to 2.5 mm) ranges from 0.8 mm (EU-LCT) up to 3.5 mm (LHD-OV). The tube mill method is used to form conduit from a variety of metals, including copper, titanium, Incoloy 908, and austenitic steels of different composition. A list of selected *CICCs* sheathed by a tube mill is given in Table 2 (95). Some cross sections of *CICCs* jacketed in tube mill are shown in Fig. 24.

Quality control of the weld (59) is obtained through tight monitoring of the process parameters. The presence of the strand bundle underneath the weld seam precludes a check by X rays or eddy currents after compacting and shaping. Stop and restart of the process (e.g., to replace the *TIG* electrode and the gas bottles) is common practice for the tube mill method.

The Pullthrough Method. In the pullthrough method (see scheme in Fig. 25) the sheath is first manufactured as a straight, oversize conduit of the same length of the final conductor section. In a second step, the bundle, wrapped with a protective metal foil, is pulled through the oversize conduit. Eventually, the conduit–cable assembly is compacted by rolling or drawing and coiled on a take-up reel.

The pullthrough method can be applied to any conduit geometry; however, it is especially attractive for thick-walled conduit and conduit with nonconstant wall thickness (which cannot be welded in a tube mill). Compared to the tube mill, an advantage of the pullthrough method is that the welds of the conduit can be fully inspected (and repaired) before assembling the superconductor.

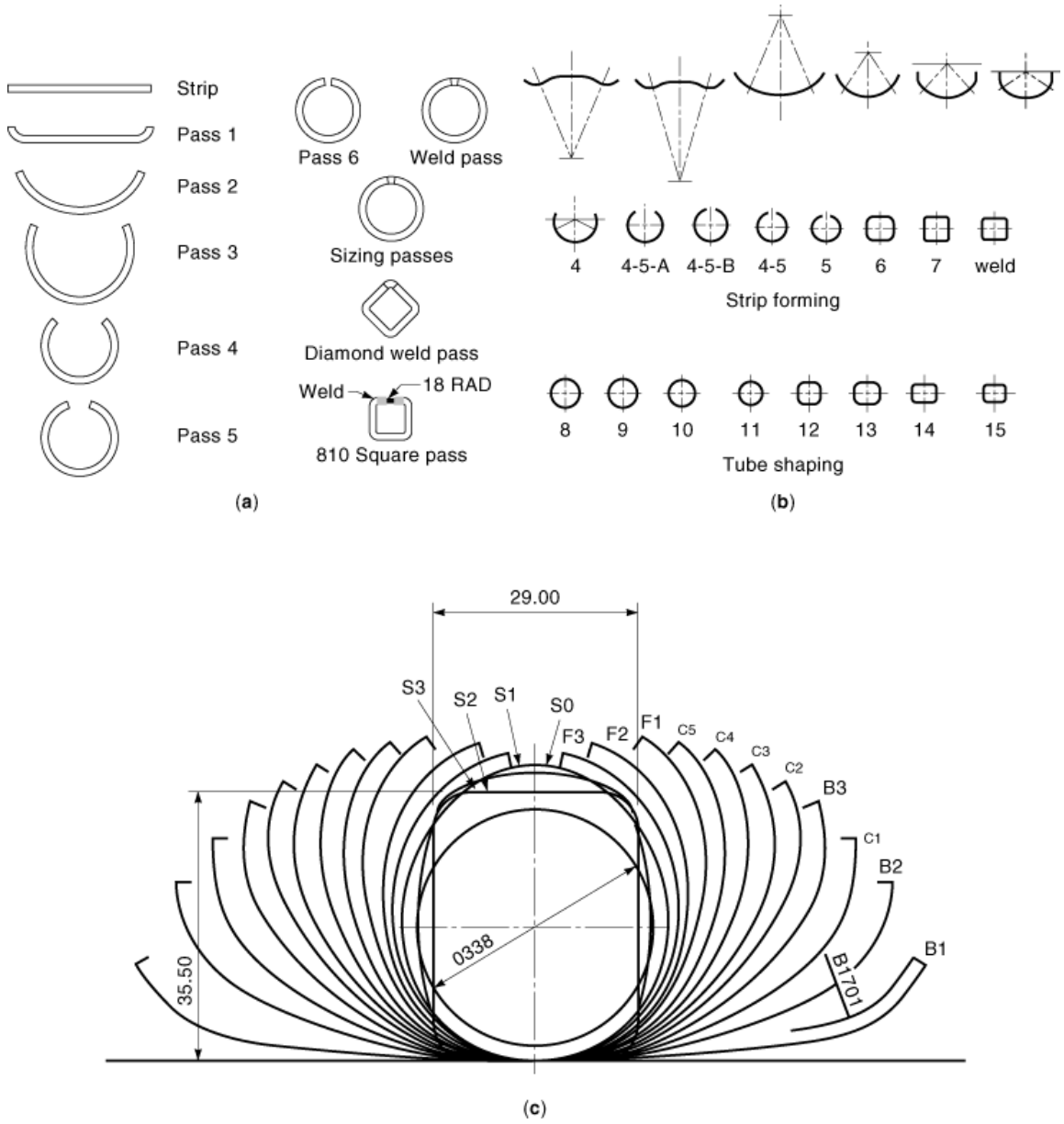

Fig. 23. The forming steps for the metal strip in a tube mill: (a) the WH-LCT (courtesy of P. Sanger); (b) the 45 T hybrid (courtesy of J. Miller); (c) the *DPC*-U (courtesy of JAERI).

The straight, oversize conduit can be assembled by different methods, including longitudinal welding of strips or profiles. However, all the pullthrough applications to date have used the butt welding of extruded tubing sections (typical unit length 6 m to 12 m). In one case (96), the 1 mm thick Incoloy 908 pipe was first manufactured in a tube mill, then cut in 10 m sections, and eventually reassembled by butt welding at the jacketing site. The pullthrough method was first applied for short conductor length and prototype conductors

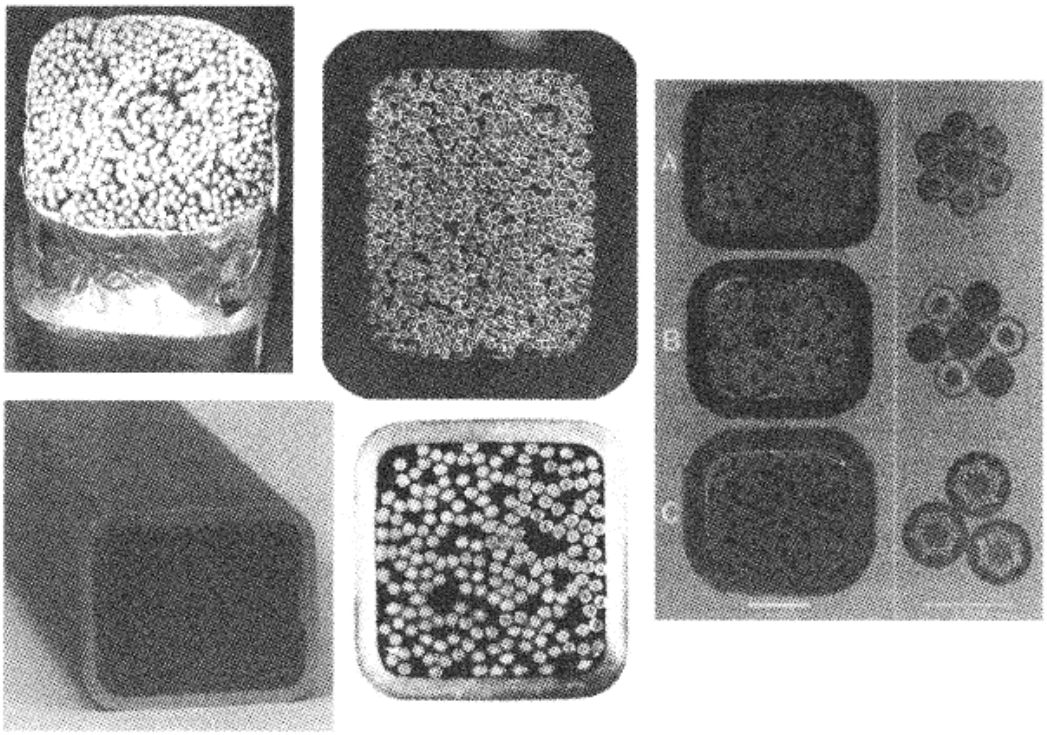

Fig. 24. Examples of *CICCs* jacketed in a tube mill: top left, the WH-LCT (94); top middle, the LHD-IV (courtesy of NIFS); bottom left, the *DPC*-U (courtesy of JAERI); bottom middle, the JF-30 (courtesy of JAERI); right, the 45 T hybrid conductors (courtesy of NHMFL).

Table 2. A Selection of CICCs Jacketed by the Tube Mill Method

Conductor	Ref.	Outer Size (mm)	Wall Thickness (mm)	Conduit Material
WH-LCT	44	20.7 × 20.7	1.73	Superalloy—JBK-75
DPC-TJ	54	17 × 22.5	1.0	Steel—316 L
LHD-OV	55	27.5 × 31.8	3.5	Steel—316 L
LHD-IV/IS	55	23.0 × 27.6	3.0	Steel—316 L
SMES—200 kA	61	51 diam	1.25	Steel—304 LN
SMES-ISTEC	37	25.4 × 27.8	2.3	Steel—316 L
US-DPC	46	22.3 × 22.3	2.45	Incoloy 908
JF-30	81	35 × 35	2.0	Steel—??
HT-7U	63	17.4 × 17.4	1.5	Steel—316 L
EU-LCT	23	10 × 40.0	0.8	Steel—316 LN
DPC-EX	33	9.4 × 40.0	1.5	Steel—JK1
HFTF	77	20.7 × 20.7	1.7	Steel—Nitronic 40
ITER—Nb_3Al insert	95	45.7 diam	2.0	Steel—Mod. JN1
12 T TF pancake	79	15.7 × 18.3	1.0	Steel—316 L
DPC-U	58	29 × 35.5	2.0	Steel—JN1
45 T hybrid—A	59	16.2 × 13.7	1.65	Steel—316 LN
45 T hybrid—C	59	15.9 × 13.7	2.0	Steel—316 LN

(e.g., Refs. 30,60). Table 3 reports the pullthrough jacketing applications with useful (>50 m) conductor length. Except for the ITER-CS conductor, the conduits quoted in Table 3 have constant wall thickness.

The butt welding of the thin-wall conduits (≤2 mm) is done with a *TIG* single-pass orbital welder without filler. A second pass with filler was necessary for the 3 mm thick conduit of GEM (85). For the circle-in-square

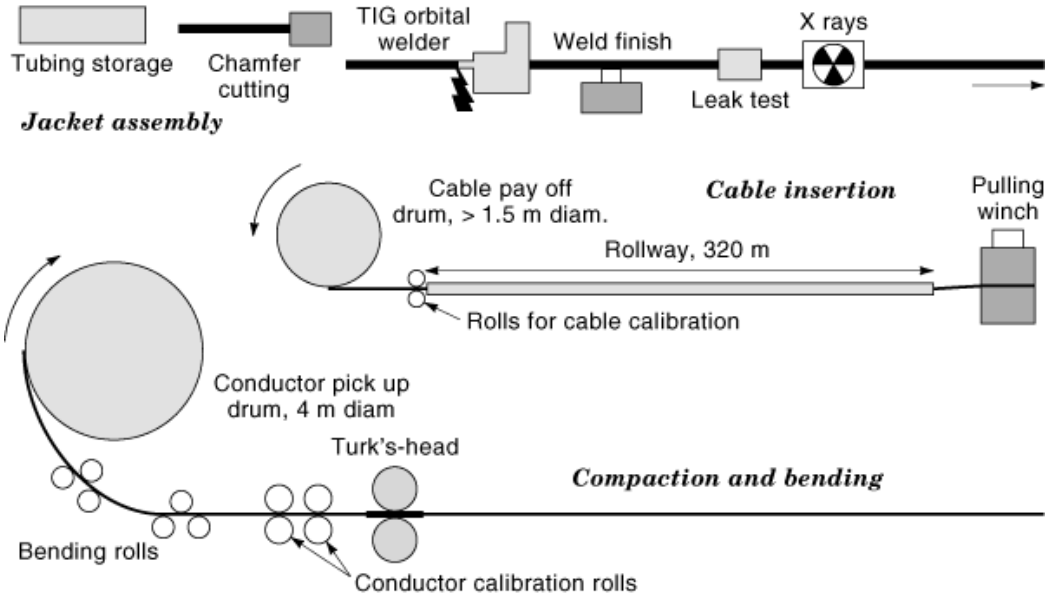

Fig. 25. Scheme of a jacketing process according to the pullthrough method.

Table 3. Long CICCs Jacketed by the Pullthrough Method

Conductor	Ref.	Outer Size (mm)	Wall Thickness (mm)	Largest Unit Length (m)	Conduit Materia
ITER-CS	53	51 3 51	6–16	200	Incoloy 908
ITER-dummy	96	39.5 diam	1	850	Incoloy 908
ITER-TF	76	40.7 diam	1.6	180	Steel—316 LN
GEM[a]	85	26.08 diam	3.05	75	Steel—304 L
ENEA-12T[b]	75	13.8 3 13.8	1.3	260	Steel—316 LN
MHD—Italy	80	16.3 3 16.3	2	340	Steel—316 LN

[a] Without the outer Al cladding.
[b] The same conductor is manufactured with sections up to 400 m long for KSTAR model coil.

Incoloy tubing of ITER-CS, a number of orbital passes with filler were carried out after the first root pass. Eventually, the corner area was filled manually. Special attention has to be paid to the weld protrusions (drops) inside the conduit: these can be monitored either by an endoscope or by inserting a calibrated gauge. The quality assurance on the butt welds may include X rays, ultrasound, dye penetrant, and leak tightness.

The applicable pulling load, F_p, is limited by the yield strength of the cable (i.e., the threshold σ_d where strand damage occurs) and by the strength of the conduit, which must react the pulling load at the insertion point (this is an issue only for thin-walled jackets). The pulling load per unit length has been found (96) to be a function of the clearance between the cable and the oversize conduit. The coefficient of friction, ν, defined as the pulling load divided by the cable weight can also be monitored. There is broad agreement (53,75,76,96)

that the insertion clearance must be larger than 1.5 mm for friction coefficients $\nu < 1$. However, according to the actual tolerance on the size of cable and conduit, a larger clearance may be necessary. The longer the conductor section to be jacketed, the more crucial becomes the issue of clearance. For short length, the risk of higher friction may be accepted. For long section jacketing, high initial friction may lead to an avalanche effect and the cable may eventually get stuck in the conduit (76).

After pullthrough, the conductor is compacted by rolling or drawing to suppress the insertion clearance. For conduits with nonconstant wall thickness, large cross-section reduction should be avoided to keep tight tolerance in the final conductor geometry. On the other hand, the compaction must achieve a positive engagement of cable and conduit to restrain strand movement in operation, which may result in dangerous instabilities.

The jacketing of long sections of CICC by the pullthrough method has been successfully demonstrated at VNIIKP, Moscow, where a 1 km long jacketing line has been set up and operated (96). The maximum conductor length $L_{\max}$ that can in principle be jacketed by the pullthrough method can be assessed by imposing the constraint that the pulling load at the head of the cable does not exceed the tensile cable strength where strand damage occurs, σ_{d} :

$$L_{\max} \leq \frac{\sigma_{\mathrm{d}}}{\nu\rho}$$

where ρ is the density of the cable, typically in the range of 7×10^3 kg/m^3 to 8×10^3 kg/m^3. The range of σ_{d} depends on the cable pattern and strand properties. For the friction coefficient ν, a safety margin must be considered. Assuming, conservatively, $\sigma_{\mathrm{d}} = 50$ MPa and $\nu \leq 1$, the maximum allowed length would be about 700 m.

Laser Beam Welding. CO_2 laser beam welding was proposed in 1986 (97) as an effective method to form thick conduit by longitudinal welding. The laser beam allows deep penetration and continuous joining with negligible deformation of thick-walled conduits in a single pass, without filler. Due to the small heat load on the underlying cable, laser welding can be applied to the final conductor size without the final compaction and shaping steps, which are mandatory in the pullthrough method and in most tube mills to suppress the gaps between cable and welded conduit. Compared to the electron beam, also used for narrow welding of thick walls, the laser beam is most suitable for continuous processes, as it does not need a vacuum environment.

Conduit segments with variable wall thickness can be manufactured by hot rolling and cold drawing in sections up to about 20 m, butt-welded and coiled to the required conductor length. Two longitudinal welds are required to join the jacket segments, with the cable fed in between, as in the tube mill. This can be obtained either by two synchronized laser beams or by a single, optically split beam. For a process rate in the range of 2 m/min, the required beam power is about 1 kW per millimeter of wall thickness. The penetration depth of the seam can be controlled in practice to $\pm 10\%$ (mostly due to the plasma oscillations in the weld). To guarantee full penetration of the weld and avoid contact of the strand bundle with the laser beam, protection underneath the weld is mandatory: this can be either a wrap on the cable or a longitudinal strip or gap under the seam.

Longitudinal laser beam welding has been applied only to two conductors: Polo (64) and the NET-ABB prototype conductors (48). The jacket of Polo is built from four quadrant profiles (see Fig. 18), preassembled by laser welding into two U profiles and eventually welded by two synchronized beams on the wrapped cable. The weld seam is 1.5 mm thick. Four conductor sections, each 150 m long, have been produced. The actual welding time for one section was less than 1 h, with several stops and restarts (97). Eddy currents were used to check the quality of the welds. Leaking spots were repaired by *TIG* welding.

In the NET-ABB prototype conductor (see Fig. 20) the weld seam is 3.9 mm thick. An air gap and a longitudinal steel strip underneath the weld protect the strand bundle from the contact with the beam. Quality assurance by ultrasound can be applied online in the process.

Despite the satisfactory employment and attractive features of laser beam welding (high rate, no deformation, minimum heat load for large penetration depth), no further application of it has been reported for

CICC jacketing in the last decade. The main reasons are the investment cost for the laser device, which can be justified only for large series production, and the limited experience of industrial conductor suppliers with the laser welding technology (a similar situation to that for lattice braiding; see above).

The Coextrusion Method. Because of the need for temperature compatibility, only aluminum alloys (see above) can be used to jacket a CICC by the coextrusion method. For the W7-X (56), the square, coextruded conduit fulfils at once the functions of helium containment, structural support, and stabilization; see Fig. 21. In the case of the GEM conductor (85), the pure Al cladding is coextruded on the steel jacketed conductor and has only the function of limiting the hot spot temperature in case of quench.

Double Conduit. To avoid the problem of assembling a thick-walled jacket, a *double conduit* has been used in a few cases. The additional conduit has no helium containment function, but its cross section adds to the main conduit from the structural point of view.

The secondary conduit may be inside the main conduit, as in the US-*DPC* [see Fig. 17(a)], where a 1 mm thick Incoloy 908 strip is formed in a tube mill and welded (not helium-tight) on the round cable (46). The inner conduit stabilizes the shape of the cable, defines the void fraction, and protects the cable during the welding of the thicker, outer conduit. During the development of the Polo conductor (64) (Fig. 18), an inner conduit with punched holes was initially foreseen as a protection for the cable during the outer conduit welding (the inner conduit was later replaced by a double wrap).

An outer secondary conduit can be used to give a structural reinforcement and provide a better shape for winding. This possibility is of special interest when the primary conduit is made in a tube mill, with constant wall thickness and large corner radii. In the MIT test conductor (82), both primary and secondary conduits are aluminum (see Fig. 21): the two extruded U profiles are fitted to the round NbTi conductor without welding. In the *DPC*-TJ (99) (see Fig. 15), the Nb_3Sn conductor, jacketed in a tube mill, pancake-wound, and heat-treated, is eventually encased and spot welded into two steel U profiles (preformed armor). The thin-walled, sharp-cornered U profiles are manufactured by 3-D milling a spiral into a thick steel plate, in order to fit the shape of the heat-treated pancake.

Choice of Manufacturing Methods

The conductor layout, and hence the manufacturing methods, are to large extent dictated by design considerations. However, the cost and the reliability of the manufacturing process should also be taken into account in the selection of the conductor layout.

Cable-in-conduit conductors are today more popular than soldered conductors, although many applications actually do not require the special features of the CICC. From the manufacturing point of view, a soldered conductor (e.g., a layer of NbTi strans cabled and soldered on a square copper pipe) is preferable and cheaper for low operating current and overall cross sections smaller than 60 mm^2. On the other hand, a CICC is more effective for high current and cross sections larger than 100 mm^2.

For cable-in-conduit conductors, a strand coating is mandatory whenever low ac loss is required, but may be omitted for dc-operated conductors. The electroplated Cr coating is the only practical choice for Nb_3Sn strands. More options are available for NbTi strands, including hot dipping in low-melting alloys and galvanic coating with Ni or Cr.

The requirement of transposition is applied currently to all the strand bundles for *CICCs*. However, nontransposed cables have been successfully operated in dc mode. An attractive, cost-saving option is to cable a layer of strands on a central copper core as the first cable stage, reducing the copper ratio in the strands and hence the overall mass of superconducting strand, and saving one cabling stage compared to the multiple-triplets pattern. Lattice braids have proved to be an elegant and effective method for strand bundling, but require the use of dedicated machinery.

The most popular conduit material for CICC is low-carbon stainless steel (nitrogen-alloyed, whenever required), readily available in any shape, easy to weld, and cheap. For Nb_3 Sn conductors, the Incoloy 908, due to the matching coefficient of thermal expansion, offers a superior performance at high field and competing mechanical properties. The higher cost, the precautions to be taken at welding and heat treating, and the single-source supplier to some extent balance the advantages of the Incoloy 908 over stainless steel.

The tube mill is a highly developed industrial process for pipe production. For *CICCs* with thin, constant-thickness conduits, the tube mill is the cheapest, easiest jacketing method, with virtually no limit on the conductor length. For thick-walled conduit, as well as for nonconstant thickness, the tube mill and *TIG* welding can be replaced by laser beam longitudinal welding of preassembled profiles. The pullthrough method, definitely preferable for prototypes and short-length jacketing because of the small investment and the low risk, has become unexpectedly popular also for long length and series production, where its competitiveness is questionable.

Three decades of forced flow superconductors show clearly a trend toward easy, low-technology manufacturing methods despite the successful demonstrations of sophisticated layouts and advanced technology (e.g., EU-LCT and Polo). Initially, the research institutes were the leaders in conductor development. Today, many companies can supply forced flow superconductors without the support of design and R&D activities from the lab community.

BIBLIOGRAPHY

1. H. H. Kolm, A closed loop cooling system for superconducting bubble chamber magnets, *Proc. Int. Symp. Magn. Technol.*, Stanford, CA, 1965, p. 611.
2. M. Morpurgo, The design of the superconducting magnet for the "OMEGA" project, *Part. Accel.*, **1**: 255, 1970.
3. M. Morpurgo, Construction of a superconducting test coil cooled by helium forced circulation, CERN Report 68-17, 1968.
4. M. Morpurgo, A superconducting solenoid cooled by forced circulation of supercritical helium, CERN Report 69-25, 1969.
5. C. Lesmond, J. C. Lottin, S. Shimamoto, Experiment with hollow conductor superconducting magnet, *Proc. Magn. Technol. Conf.*, Hamburg, 1970, Vol. 3, p. 925.
6. G. Meyer R. Maix, Superconductors and superconducting magnets, *Brown Boveri Rev.*, **57**(7/8): 355, 1970.
7. Y. Naganuma, *et al.* The manufacture of hollow superconductors, *Proc. ICEC*, Kyoto, 1974, Vol. 5, p. 508.
8. V. N. Agureev, *et al.* Electroplated stabilized multifilament superconductor, *IEEE Trans. Magn.*, **11**: 303, 1975.
9. D. P. Ivanov et al Test results of "tokamak-7" superconducting magnet system (SMS) sections, *IEEE Trans. Magn.*, **15**: 550, 1979.
10. E. Yu. Klimenko et al, Superconducting conductor for T-15 toroidal magnet, *Sov. At. Energy (Engl. Transl.)*, **63**: 756, 1987.
11. N. Schaetti, Superconductors for the magnet coils of the Omega spark chamber at CERN, *Brown Boveri Rev.*, **59** (2/3): 73, 1972.
12. M. Morpurgo, A large superconducting dipole cooled by forced circulation of two phase helium, *Cryogenics*, **19**: 411, 1979.
13. H. Hillmann, Fabrication technology of superconducting material, in S. Foner and B. B. Schwartz, (eds.), *Superconductor Material Science*, Ser. B68, New York: 1981. NATO Adv. Study Inst., 1981.
14. G. Pasotti, *et al.* SULTAN: An 8 T, 1 m bore test facility, the outer solenoid, *IEEE Trans. Magn.*, **17**: 2007, 1981.
15. U. Trinks, *et al.* A protoype coil for the superconducting separated sector cyclotron SuSe, *J. Phys., Cl. Suppl. 1*, **45**: 217, 1984.
16. K. Agatsuma, *et al.* Braided multifilamentary Nb_3 Sn hollow superconductor and its magnet, *IEEE Trans. Magn.*, **15**: 787, 1979.
17. H. Benz, *et al.* The conductor for the Swiss LCT coil, *IEEE Trans. Magn.*, **17**: 2213, 1981.
18. H. Benz, *et al.* Design and manufacture of the conductor for the Swiss LCT coil, *IEEE Trans. Magn.*, **19**: 711, 1983.

19. W. M. P. Franken, *et al.* Manufacture of the hollow supercritical He cooled conductor for the ECN/SULTAN project, *IEEE Trans. Magn.*, **19**: 368, 1983.
20. B. Jakob G. Pasztor, Fabrication of a high current Nb_3 Sn forced flow conductor for the 12 tesla SULTAN test facility, *IEEE Trans. Magn.*, **23**: 914, 1987.
21. J. A. Roeterdink, *et al.* Design and construction of the ECN 12 T niobium tin magnet insert for the SULTAN facility, *IEEE Trans. Magn.*, **24**: 1429, 1988.
22. B. Jakob, G. Pasztor, R.G. Schindler, Fabrication of high current Nb_3 Sn forced flow conductors and coils for the SULTAN III test facility, *Fusion Techology 1992*, Amsterdam: Elsevier, 1993, p. 872.
23. H. Krauth, *et al.* Manufacturing and testing of a forced flow cooled superconductor for tokamak magnets, *IEEE Trans. Magn.*, **17**: 918, 1981.
24. H. Krauth, *et al.* Development and testing of a forced flow cooled superconductor for LCT, *Proc. 8th Symp. Eng. Probl. Fusion Res.*, 1979, p. 1451.
25. B. Jakob, *et al.* Design and fabrication of a 17 kA preprototype Nb_3 Sn conductor for the Tf coils of the NET fusion project, *IEEE Trans. Magn.*, **24**: 1437, 1988.
26. J. M. Plaum, *et al.* Development toroidal field conductor for NET, *IEEE Trans. Magn.*, **24**: 1433, 1988.
27. R. Flükiger, *et al.* The Nb_3 Sn react and wind conductor for NET toroidal field coils and its boundaries, *Fusion Technology 1990*, Amsterdam: Elsevier, 1991, p. 1584.
28. V. A. Glukhikh, Programme of the conductor development for the ITER toroidal field coils, *Proc. Magn. Technol. Conf.*, Tsukuba, 1989, Vol. 11, p. 886.
29. K. Agatsuma, *et al.* Fabrication and test of a forced cooled Nb_3 Sn superconducting coil, *IEEE Trans. Magn.*, **21**: 1040, 1983.
30. K. Agatsuma, *et al.* Stainless steel sheathed forced internally cooled Nb_3 Sn superconductor and its coil test, *IEEE Trans. Magn.*, **23**: 1535, 1987.
31. T. Ando, *et al.* +2 T test module coil (*TMC*-II) in the cluster test program, *Proc. 10th Symp. Fusion Eng.*, Philadelphia, 1983, p. 1346.
32. M. Sugimoto, *et al.* Development of hollow cooling monolithic conductor for ITER TF coil, *IEEE Trans. Magn.*, **28**: 218, 1992.
33. T. Ando, *et al.* Fabrication and test of the Nb_3 Sn demo poloidal coil (*DPC*-EX), *Fusion Technology 1990*, Amsterdam: Elsevier, 1991, p. 243.
34. H. Nakajima, *et al.* Tensile properties of new cryogenic steels as conduit material for forced flow superconductors at 4 K, *Adv. Cryog. Eng. Mater.*, **34**: 173, 1988.
35. M. D. Sumption, *et al.* Contact resistance and cable loss measurements of coated strands and cables wound from them, *IEEE Trans. Appl. Supercond.*, **5**: 692, 1995.
36. J. M. Depond, *et al.* Examination of contacts between strands by electrical measurement and topographical analysis, *IEEE Trans. Appl. Supercond.*, **7**: 793, 1997.
37. T. Satow, *et al.* Present status of 480 MJ/40 MW SMES development project, *Proc. Int. Conf. Electr. Eng.*, Matsue, Japan, 1997.
38. K. Kwasnitza, A. Sultan, S. Al-Wakeel, AC losses of a 10 kA NbTi cable-in-conduit superconductor for SMES application, *Cryogenics*, **36**: 27, 1996.
39. K. Takahata, *et al.* Stability tests of the NbTi cable-in-conduit superconductor with bare strands for demonstration of the large helical device poloidal field coils, *IEEE Trans. Magn.*, **30**: 1705, 1994.
40. G. Pasztor, *et al.* Design fabrication and testing of a 100 kA superconducting transformer for the SULTAN test facility, *Proc. Magn. Technol. Conf.*, Beijing, 1997, Science Press, 1998, Vol. 15, p. 839.
41. Y. Takahashi, *et al.* Experimental results of stability and current sharing of NbTi cable-in-conduit conductors for the poloidal field coils, *IEEE Trans. Appl. Supercond.*, **3**: 610, 1993.
42. J. E. C. Williams, *et al.* The development of a NbTi cable-in-conduit coil for a 45 T hybrid magnet, *IEEE Trans. Magn.*, **32**: 1633, 1994.
43. K. Okuno, *et al.* Ac loss performance of 1 m bore, large-current Nb_3 Sn superconducting coils in JAERI demo poloidal coil project, *IEEE Trans. Appl. Supercond.*, **3**: 602, 1993.
44. C. J. Heyne, *et al.* Westinghouse design of a force flow Nb_3 Sn test coil for the large coil program, *Proc. 8th Symp. Eng. Probl. Fusion Res.*, San Francisco, 1979, p. 1148.
45. N. Aoki, *et al.* Development of forced-cooled Nb_3 Sn bundle conductor, *IEEE Trans. Magn.*, **19**: 733, 1983.

46. M. M. Steeves, *et al.* The US demonstration poloidal coil, *IEEE Trans. Magn.*, **27**: 2369, 1991.
47. B. J. P. Baudouy, *et al.* AC loss measurements of the 45 T hybrid/CIC conductor, *IEEE Trans. Appl. Supercond.*, **5**: 689, 1995.
48. P. Bruzzone, Fabrication of a short length of wind and react conductor, ASEA Brown Boveri Rep. HIM 20420, Zurich, 1990.
49. Y. Ipatov, *et al.* Galvanic chrome plating of copper wire for the ITER program. *Proc. ICEC/ICMC 96*, Kitakyushu, Japan, Elsevier, 1996, 1969.
50. P. Bruzzone, A. Nijhuis, H. H. J. ten Kate, Effect of Cr plating on the coupling current loss in cable-in-conduit conductors, *Proc. ICEC/ICMC 96*, Kitakyushu, Japan, Elsevier, 1996, p. 1243.
51. Y. Ipatov, P. Dolgosheev, V. Sytnikov, Prospective barrier coatings for superconducting cables, *Supercond. Sci. Technol.*, **10**: 507, 1997.
52. K. Kwasnitza I. Horvath, Experimental evidence for an interaction effect in the coupling losses of cabled superconductors, *Cryogenics*, **23**: 9, 1983.
53. P. Bruzzone, *et al.* Conductor fabrication for the ITER model coils, *IEEE Trans. Magn.*, **32**: 2300, 1996.
54. N. Aoki, *et al.* Fabrication of superconductor for the *DPC*-TJ coil, *Cryogenics*, **33**: 581, 1993.
55. K. Nakamoto, *et al.* Design and fabrication of forced-flow superconducting poloidal coils for the Large Helical Device, *Fusion Technology 1994*, Amsterdam: Elsevier, 1995, p. 909.
56. R. Heller, Superconductor for the coils of the modular stellarator Wendelstein 7-X, *IEEE, Trans. Magn.*, **30**: 2383, 1994.
57. J. V. Minervini, *et al.* Conductor design for the GEM detector magnet, *Proc. IISSC*, San Francisco, 1993, Vol. 5, p. 595.
58. T. Kumano, *et al.* Development of superconductors for the DEMO poloidal coils (*DPC*-U1, U2), *Proc. Magn. Technol. Conf.*, Tsukuba, 1989, Vol. II, p. 841.
59. J. R. Miller, *et al.* Experience on sheathing 10 km of cable-in-conduit conductor for the NHMFL hybrid, *Adv. Cryog. Eng. Mater.*, **41**: 489, 1996.
60. D. Bessette, *et al.* Fabrication and test results of the 40 kA CEA conductors for NET/ITER, *Fusion Technology 1992*, Amsterdam: Elsevier, 1993, p. 788.
61. D. L. Walker, *et al.* Design of a 200 kA conductor for superconducting magnetic energy storage (*SMES*), *Adv. Cryog. Eng.*, **35**: 573, 1990.
62. A. Anghel, *et al.* The ITER quench experiment on long length at the SULTAN facility, *Fusion Technology 1994* Amsterdam: Eberier, 1995, p. 881.
63. B. Z. Li, *et al.* Conductor fabrication for the HT-7U model coil, *Fusion Technology 1998*, Amsterdam: Elsevier, 1998, p. 775.
64. S. Förster, U. Jeske, A. Nyilas, Fabrication of a 15 kA NbTi cable for the 150 T/s high ramp rate polo model coil, *Fusion Technology 1988*, Amsterdam: Elsevier, 1989, p. 1557.
65. R. Heller, *et al.* Stability of a poloidal field coil under rapidly changing magnetic field, *IEEE Trans. Magn.*, **32**: 2336, 1996.
66. M. A. Janocko, Lattice braided superconductors, *IEEE Trans. Magn.*, **15**: 797, 1979.
67. P. Bruzzone, Fully transposed braids for the prototype cable-in-conduit conductors of NET, *IEEE Trans. Magn.*, **28**: 190, 1992.
68. P. Bruzzone, N. Mitchell, J. Kübler, Mechanical behavior under transversal load of the 40 kA Nb_3 Sn cable-in-conduit conductor for the NET inner poloidal coil, *Proc. Magn. Technol. Conf.*, Tsukuba, 1989, Vol. 11, p. 926.
69. C. R. Walters, *et al.* Quench transients in internally cooled conductors, *IEEE Trans. Magn.*, **19**: 680, 1983.
70. M. Shimada S. Tone, Effect of niobium on cryogenic mechanical properties of aged stainless steel, *Adv. Cryog. Eng.*, **34**: 131, 1988.
71. J. Kübler, H. J. Schinder, W. J. Muster, Influence of aging on the fracture toughness of cryogenic austenitic materials, evaluated by a simple method, *Adv. Cryog. Eng. Mater.*, **38**: 191, 1992.
72. R. P. Reed, R. P. Walsh, C. N. McCowan, Effect of Nb_3 Sn heat treatment on the strength and toughness of 316 LN alloys with different carbon content, *Adv. Cryog. Eng. Mater.*, **38**: 45, 1992.
73. H. Nakajima, *et al.* Development of high strength austenitic stainless steel for conduit of Nb_3 Al conductors, *Adv. Cryog. Eng.*, **42**: 323, 1996.
74. R. P. Walsh, L. T. Summers, J. R. Miller, The 4 K tensile and fracture toughness properties of a modified 316LN conduit alloy, *Proc. ICEC/ICMC 96*, Kitakyushu, Japan, Elsevier, 1996, p. 1891.

75. R. Bruzzese, *et al.* The cable-in-conduit Nb_3 Sn conductor for the EURATOM-ENEA 12 T wind-and-react magnet, *IEEE Trans. Appl. Supercond.*, **3**: 515, 1993.
76. A. della Corte, *et al.* Successful completion of the conductor manufacture for the ITER-TF model coil, *Fusion Technology 1998*, Amsterdam: Elsevier, 1998, p. 841.
77. M. M. Olmstead M. O. Hoenig, Constructing, fabricating and forming of internally cooled cabled superconductors, *IEEE Trans. Magn.*, **17**: 922, 1981.
78. M. Nishi, *et al.* A 12 T forced flow type superconducting magnet, *IEEE Trans. Magn.*, **23**: 1531, 1987.
79. M. Yamaguchi, *et al.* Development of a 12 T forced cooling toroidal field coil, *Proc. ICEC*, **10**: 169, 1984.
80. F. Negrini, *et al.* First results of the Italian national program on superconducting MHD magnets technology, *IEEE Trans. Magn.*, **30**: 2086, 1994.
81. Y. Takahashi, *et al.* Development of a 30 kA cable-in-conduit conductor for pulsed poloidal coils, *IEEE Trans. Magn.*, **19**: 386, 1983.
82. M. O. Hoenig, A. G. Montgomery, S. J. Waldman, Experimental evaluation of a 1 m scale D-shaped test coil fabricated from a 23 m length of internally cooled, cabled superconductor, *Adv. Cryog. Eng.*, **25**: 251, 1979.
83. Machbarkeitsstudie über einen Supraleiter für Wendelstein VII-X, ABB Rep. HIM 20442, 1989.
84. H. Kronhardt, O. Dormicchi, J. Sapper, Design and manufacture of a Wendelstein 7-X demonstration coil, *Fusion Technology 1998*, Amsterdam: Elsevier, 1998, p. 735.
85. N. N. Martovetsky, *et al.* GEM detector conductor manufacturing experience, *IEEE Trans. Appl. Supercond.*, **5**: 761, 1995.
86. R. E. Gold, *et al.* Evaluation of conductor sheath alloys for a forced flow Nb_3 Sn superconducting magnet coil for the large coil program, *Adv. Cryog. Eng. Mater.*, **28**: 759, 1982.
87. I. S. Hwang, *et al.* Mechanical properties of Incoloy 908—an update. *Adv. Cryog. Eng. Mater.*, **38**: 1, 1992.
88. A. Bussiba, R. L. Tobler, J. R. Berger, Superconductor conduits: Fatigue crack growth rate and near threshold behavior of three alloys. *Adv. Cryog. Eng. Mater.*, **38**: 167, 1992.
89. W. Specking, J. L. Duchateau, P. Decool, First results of strain effects on critical current of Incoloy jacketed Nb_3 Sn CICC's, *Proc. Magn. Technol. Conf.*, Beijing, 1997, Science Press, 1998, Vol. 15, p. 1210.
90. J. S. Smith, J. H. Weber, H. W. Sizek, Control of stress-accelerated oxygen assisted cracking of Incoloy alloy 908 sheath for Nb_3 Sn cable-in-conduit, *Adv. Cryog. Eng.*, **42**: 407, 1996.
91. N. Mitchell, *et al.* Avoidance of *SAGBO* in Incoloy^R 908 used as a jacket material for Nb_3 Sn conductors, *Proc. Magn. Technol. Conf.*, Beijing, 1997, Science Press, 1998, Vol. 15, p. 1163.
92. J. H. Weber J. M. Poole, Production and properties of Incoloy^R alloy 908 tubing for sheathing of Nb_3 Sn superconducting cables, *Adv. Cryog. Eng.*, **42**: 383, 1996.
93. H. Nakajima, *et al.* 4 K mechanical properties of pure titanium for the jacket of Nb_3 Sn superconductors, *Proc. ICEC/ICMC 96*, Kitakyushu, Japan, Elsevier, 1996, p. 1895.
94. P. Sanger, *et al.* The trials and tribulations of fabricating the pipe for the "rope-in-pipe" Nb_3 Sn superconductor, *Adv. Cryog. Eng.*, **28**: 751, 1982.
95. N. Koizumi, *et al.* Design of the Nb_3 Al insert to be tested in ITER central solenoid model coil, *IEEE Trans. Magn.*, **32**: 2236, 1996.
96. V. Sytnikov, *et al.* RF jacketing line for manufacturing ITER cable-in-conduit conductor, *Proc. ICEC/ICMC 96*, Kitakyushu, Japan, Elsevier, 1996, p. 799.
97. S. Förster, *et al.* Development of components for poloidal field coils within the KFK Polo project, *Fusion Technology 1990*, Amsterdam: Elsevier, 1991, p. 1706.
98. R. Garré, *et al.* Development and manufacture of superconducting cable-in-conduit conductors, *Cryogenics*, **34** (Suppl.): 619, 1994.
99. M. Nishi, *et al.* Development of high current density, large superconducting coil for fusion machines: The *DPC*-TJ program, *Cryogenics*, **33**: 573, 1993.

PIERLUIGI BRUZZONE
Centre de Recherches en Physique des Plasmas